Universidade de Lisboa

Faculdade de Farmácia

Lignin Nanoparticles for Cancer Therapy

Cláudio Alexandre Rodrigues Ferro

Mestrado Integrado em Ciências Farmacêuticas

Lisboa, 2017

Faculdade de Farmácia

Universidade de Lisboa

Lignin Nanoparticles for Cancer Therapy

Cláudio Alexandre Rodrigues Ferro

Monografia de Mestrado Integrado em Ciências Farmacêuticas apresentada à Universidade de Lisboa através da Faculdade de Farmácia

Orientador: **Professor Auxiliar Helena F. Florindo, Departamento de Farmácia Galénica e Tecnologia Farmacêutica, Faculdade de Farmácia, Universidade de Lisboa**

Lisboa, 2017

Faculty of Pharmacy
University of Helsinki

School of Chemical Engineering
Aalto University

Faculdade de Farmácia
Universidade de Lisboa

Supervisors: **Patrícia Figueiredo and Associate Professor Hélder A. Santos, Drug Research Program, Division of Pharmaceutical Technology, Faculty of Pharmacy, University of Helsinki, Finland**

Co-Supervisors: **Associate Professor Mauri Kostiainen, Research Group of Biohybrid Materials, School of Chemical Engineering, University of Aalto, Finland**

Assistant Professor Helena F. Florindo, Department of Pharmaceutics and Pharmaceutical Technology, Faculdade de Farmácia, Universidade de Lisboa

This Monography was entirely publish in a scientific article:

Figueiredo P, Ferro C, Kemell M, Liu Z, Kiriazis A, Lintinen K, et al. Functionalization of carboxylated lignin nanoparticles for targeted and pH-responsive delivery of anticancer drugs. Nanomedicine (Lond) [Internet]. 2017. Available from: http://dx.doi.org/10.2217/nnm-2017-0219

Abstract

Recently, lignin has been used as a starting material for the development of nanoparticles (NPs) for different purposes, including for biomedical applications. In this study, the carboxylation of the native lignin was carried out towards the modification of carboxylated lignin NP (CLNPs) with a block copolymer made of poly(ethylene glycol) (PEG), poly(histidine) (PHIS) and cell-penetrating peptide (CPP). The success of the conjugation reactions was confirmed by the conversion of the zeta-potential (ζ-potential) values from negative values for the bare CLNPs to positive values after the surface functionalization. The prepared CLNPs showed spherical shape, good size distribution, moderate polydispersity, good stability in physiological media and low cytotoxicity in all the tested cell lines at a concentration up to at least 250 µg/mL, after 24 h of incubation. A poorly water-soluble cytotoxic agent, benzazulene (BZL), was loaded into the CLNPs, improving its release profiles at pH 5.5 and 7.4. Furthermore, the release of BZL was found to be pH-sensitive, with higher release rates at pH 5.5 than at pH 7.4. Consequently, the BZL-loaded CLNPs conjugated with PEG-PHIS-CPP (BZL@CLNPs-PEG-PHIS-CPP) showed an enhanced antiproliferative effect in the different cancer cells (IC50 < 24 µM) compared to a normal endothelial cell line (IC50 ≈ 45 µM) after 24 h incubation, making the CLNPs promising candidates for anticancer therapy.

Keywords: lignin nanoparticles; targeting functionalization; drug loading; pH-responsive release; antiproliferative effect

Resumo

Recentemente, a lignina tem sido utilizada como matéria-prima para o desenvolvimento de nanopartículas para diferentes fins, incluindo para aplicações biomédicas. Neste estudo, procedeu-se à carboxilação da lignina nativa tendo em vista a modificação de nanopartículas de lignina carboxilada (CLNPs) com um copolímero constituído por poli(etilenoglicol) (PEG) e poli(histidina) (PHIS). A superfície das CLPNs também foi funcionalizada com um Péptido de Penetração Celular (CPP). O sucesso das reações de conjugação foi confirmado pela conversão dos valores negativos do potencial zeta obtido para as CLNPs puras, para valores positivos após a funcionalização da superfície destas nanopartículas. As CLNPs apresentaram forma esférica, boa distribuição de tamanhos, polidispersão moderada, boa estabilidade em meios fisiológicos e baixa citotoxicidade em todas as linhas celulares testadas em concentrações até pelo menos 250 μg/mL, após 24 h de incubação. Um agente citotóxico pouco solúvel em água, benzazulina (BZL), foi encapsulado nas CLNPs, melhorando os seus perfis de libertação a pH 5,5 e 7,4. Além disso, a libertação de BZL foi sensível ao pH, com taxas de libertação mais elevadas a pH 5,5 do que a pH 7,4. Consequentemente, as CLNPs conjugadas com PEG-PHIS-CPP contendo BZL (BZL @ CLNPs-PEG-PHIS-CPP) mostraram um efeito antiproliferativo aumentado nas diferentes células cancerígenas (IC50 <24 μM), em comparação com uma linha celular endotelial normal (IC50 ≈ 45 μM) após 24 h de incubação, o que torna as CLNPs alternativas terapêuticas promissoras para o tratamento do cancro.

Palavras chave: Nanopartículas de lignina; Funcionalização; Encapsulação de fármacos; Libertação sensível ao pH; Efeito antiproliferativo

Acknowledgments

This study was carried out at the Division of Pharmaceutical Chemistry and Technology, Faculty of Pharmacy, University of Helsinki and at the Department of Bioproducts and Biosystems, Aalto University, under the Erasmus Placement program, which agreement was made between the Faculty of Pharmacy and the Aalto University.

I wish to express my sincere gratitude first of all to Professor Hélder Santos and to Professor Mauri Kostiainen, for accepting me as Erasmus Trainee and for giving me the chance to do the research that gave rise to this monography.

I would like to thank Professor Santos for welcoming me in his team and for giving me the opportunity to work in several scientific areas. I thank him for guiding me and improving my research skills through his feedback, his constant presence and worry and for being an excellent human being that, through his attitude in the laboratory and his motivation inputs, made my passion for science grow even more.

I also thank Professor Kostiainen for being my Erasmus Supervisor, for his availability and support during all my stay in Helsinki, by his worries about the research project I was developing and for helping me to overcome any bureaucratic problems I had during my Erasmus program.

I am very grateful to Professor Helena Florindo for improving my interest in Nanotechnology, for her advices and support while I was looking for a research laboratory for realize a Erasmus Program, during my stay in Helsinki and for all the help during the realization of this work.

I would like to thank especially to the PhD student Patricia Figueiredo who accompanied me during all the research involved in this work, allowing me to collaborate in her own project. Through her positive spirit and guidance, by trusting me and allowing me to be independent, I became a more confident person in my skills as a scientist.

I also would like to thank to all the research team in the Santos' Lab, for their warm welcome, technical support and knowledge and by providing a pleasant working atmosphere, where everyone tries to help the others.

Finally, I thank my family, specially my parents, Isabel e António Ferro, for being my rock when I feel fragile and when I most need help, for their love and sacrifices made for me, for showing me the hard reality of the world, but still give me the opportunity to dream and have my own objectives and for passing me values of responsibility, sharing

and coherence. I also thank all my friends, from high-school to faculty, which support made me grow as a person and also as a professional.

Abbreviations

ATR	attenuated total reflectance
BZL	Benzazulene
CLNPs	carboxylated lignin nanoparticles
CPP	cell-penetrating peptide
DMAP	4-dimethylaminopyridine
DMEM	dulbecco's modified eagle medium
DLS	dynamic light scattering
EDC/NHS	1-ethyl-3-(3-dimethylaminopropyl) carbodiimide hydrochloride and N-hydroxysuccinimide
e.g.	*exempli gratia*
FBS	fetal bovine serum
FTIR	fourier transformed infrared spectroscopy
HBSS-HEPES	4-(2-hydroxyethyl)-1-piperazineethanesulfonic acid
HPLC	high-performance liquid chromatography
LNPs	lignin nanoparticles
MES	2-(N-morpholino)ethanesulfonic acid
MRI	magnetic resonance imaging
NPs	Nanoparticles
NT	Nanotechnology
PBS	phosphate buffer saline
PEG	poly(ethylene glycol)
PDI	polydispersity index
PDT	photodynamic therapy
PET/CT	positron emission tomography / computed tomography
P-gp	*P*-glycoprotein
pH	potential of hydrogen
PHIS	poly(histidine)
PNPs	Polymeric Nanoparticles
PSA	prostate-specific antigen
PTT	photothermal therapy
TEM	transmission electron microscopy
THF	Tetrahydrofuran
UV	ultraviolet rays
ζ-potential	zeta potential

Index

Figures Index

Table Index

1. Introduction

Conventionally, nanotechnology (NT) comprehend materials, devices and systems with the size of 1 to 100 nm, however many nanomedicines are within the submicron size of 100-1000 nm (1,2). Indeed, NT has been given new and better approaches to several diseases compared to the traditional ones (3–5). For example, NT showed to be useful for the treatment of neurodegenerative (6), autoimmune (7,8) and cardiovascular diseases (9,10), osteoporosis (11) and against bacterial infections (12). However, one of the main uses of NPs in medicine is as drug delivery systems, mainly for cancer therapy, by specifically directing NPs to target cancer cells (13,14).

Cancer is still a leading cause of diseases worldwide, with 14.1 million new cases and 8.2 million deaths in 2012. It is also expected that the burden of cancer will increase to 23.6 million new cases per year by 2030 (15–17). Despite these alerting numbers, the main therapies include surgery, radiation and chemotherapy, which have disadvantages, such as lack of specificity and effectivity (18,19). In this context, NT appears as a new and encouraging approach, due to the possibility to specifically target cancer cells, increasing the therapeutic effectivity of the chemotherapeutic agents and decreasing their side effects (3). These targeting made by the NPs can be passive or active (19). Passive targeting is based on the physiologic alterations caused by the existence of a cancer tissue, including the enhanced permeability and retention (EPR) effect, and an acidification of the environment around the cancer cells, which allows the preferable accumulation of NPs in the neoplastic tissues and the degradation of pH-sensitive NPs, respectively (20,21). In addition, active targeting promote the uptake of NPs into the cancer cells by adding specific ligands to the NPs, such as CPP, that promotes the specific targeting and the NPs internalization into the cancer cells (18,19).

Polymeric NPs (PNPs) have shown a great potential for cancer therapy, because of their capability to adsorb, encapsulate or conjugate the anticancer agent within or onto their surface. Also, their formulations include polymers that are hydrophobic, non-toxic and blood compatible and ligands that specifically target receptors overexpressed on cancer cells (22).

Lignin is a biopolymer with great potential for the preparation of NPs (23), due to its large abundance in nature (24) and its encouraging characteristics, such as biodegradability, biocompatibility, good stability and the possibility to chemically

modify its structure thanks to the presence of phenolic and aliphatic hydroxyl groups (23). At the same time, lignin nanoparticles (LNPs) demonstrated the ability to load different drugs and the possibility of being modified with targeting molecules, such as pH-sensitive polymers and targeting ligands, allowing a pH-responsive drug release and an increased cellular interaction with specific cells, respectively (23). According to this information, LNPs have shown an increasing potential to be used as delivery systems for anticancer therapy (25).

The main aim of this monography was to study the potential of CLNPs, conjugated with CPP and NH_2-PEG-PHIS as delivery systems to be used for cancer therapy. The specific aims were: (i) to synthetize carboxylated lignin and therefore prepare and characterize CLNPs; (ii) to functionalize CLNPs with the block copolymer NH_2-PEG-PHIS and CPP in order to prepare CLNPs-CPP and CLNPs-PEG-PHIS-CPP; (iii) to characterize and evaluate the size, surface charge, stability and cytotoxicity of the prepared CLNPs; (iv) to evaluate the loading of a poorly water-soluble cytotoxic compound, BZL, and its release profiles at different pH values (5.5 and 7.4); and, finally, (v) to study the antiproliferative effect of the BZL-loaded CLNPs using several cancer cell lines (breast, prostate and colorectal cancers) and a non-tumor endothelial cell line as a control.

2. Review of Literature

2.1. Biomedical Applications of Nanotechnology

Since the NT emerged, in 1958 with Richard Feyman (3) , it has being used for several applications, including the agriculture, development of transportation, space engineering and the improvement of the electronic components. However, one of the fields in which NT has most revolutionized is medicine (3,4). NT comprehend materials, devices and systems with the size of 1 to 100 nm (**Figure 2. 1**), giving them unique properties (3,5).

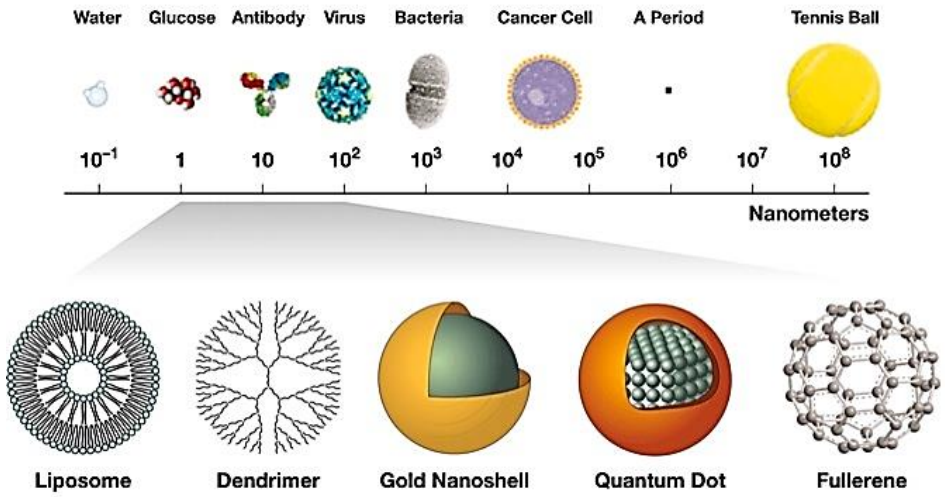

Figure 2. 1 - Nanoscale and possible Nanostructures (image copied from https://ocg.cancer.gov/e-newsletter-issue/issue-11/translating-cancer-targets-nanotechnology-based-therapeutics)

These singular properties of NT can be very useful in the treatment of several diseases such as neurodegenerative (6), autoimmune (7,8) and cardiovascular diseases (9,10) and osteoporosis (11). In the field of neurodegenerative diseases, the NT can improve the regeneration of the damaged neurons, protecting them, and enhance the delivery of specific drugs through the blood-brain barrier (3,6). For the autoimmune diseases, the NPs have been used to reverse the lack of specificity of the anti-inflammatory treatments using specific peptides that bind to molecules overexpressed in the target cell, to protect the drugs from clearance (by modification of the surfaces) or to improve the transport across physiological barriers (7). For example, the use of lipid-based NPs has been studied for multiple sclerosis due to their capacity to cross the blood-

brain barrier and the possibility to insert lipid-soluble drugs (*e.g.*, glucocorticoids) in the phospholipid membrane and the water soluble drugs (*e.g.*, mitoxantone) in the inner core (8).

NT can also be used in the diagnosis and therapy of cardiovascular diseases such as coronary artery disease (9,10), by providing molecular imaging approaches, such as the use of NPs-based fluorescence imaging or super-paramagnetic iron oxide particles in the magnetic resonance imaging (MRI) (9,10). Also, NPs attached with certain molecules showed to target specific receptors, endothelial cells or macrophages involved in atherosclerosis (9,10). Other strategies were studied, such as pH-responsive delivery of antioxidants or the use of polymeric nanocoatings in stents (10). Osteoporosis is another disease where mineral-based nanomaterials have been produced, including calcium phosphate and silica NPs, which showed promising results in the production of new bone or reverse the osteoclast activity (11). Other interesting application of NT is the tendon healing and regeneration, by increasing the drug penetration across the skin and functioning as a vector for delivering of genetic material and polysaccharides, such as chitosan (12).

NPs have also been studied in order to decrease the antimicrobial drug resistance, because of their high surface-to-volume ratio that improves their interaction with microorganisms (26). Furthermore, several NPs by themselves showed antimicrobial properties, due to their anti-adhesion capacity that decreases the production of biofilms, oxidation or reduction properties with consequent production of reactive oxygen species, and also by altering the bacterial physiology, through the generation of holes in the cell wall, for example (26). Thus, the use of NPs, in particular the inorganic NPs, is very useful for fighting superbugs (26,27). NPs have also applications in the field of vaccination (27). For example, synthetic NPs can module the activity of antigen presenting cells, by encapsulating or releasing immunomodulators that increase the dendritic cell activation, and lead to a specific immune recognition and also acting as co-adjuvants (27).

As above mentioned, one of the main uses of NT in medicine is the use of NPs as drug delivery systems, leading to the reduction of side-effects and the amount of drug used, lower costs and reduced patients' pain (3). This strategy is mainly used in cancer therapy by specifically targeting the different types of NPs (**Figure 2. 2**) to cancer cells (13,14), either by passive or active targeting (19).

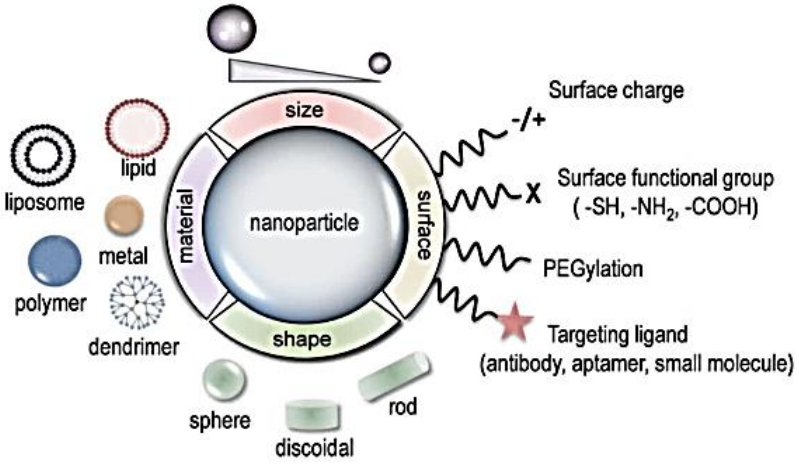

Figure 2. 2 - Possible NPs variations and changes: material, type, surface and shape (14)

Passive targeting comprehends an increase of permeability and retention of macromolecules, including NPs, that results from the lacking of smooth muscle cells, which leads to a permanent vasodilation and therefore their accumulation in the neoplastic tissues (21). However, passive targeting cannot promote the uptake of NPs by the malign tissues, what is exactly what active targeting does. Thus, active targeting comprises the selective targeting of receptors overexpressed on cancer cells by conjugating ligands onto NPs' surface, which promotes NPs' internalization by triggering receptor-mediated endocytosis (19). These ligands can be antibodies or aptamers, which are single stranded DNA or RNA that binds to specific cell proteins or peptides. Ligands can also be peptides, such as CPP, a highly cationic peptide, composed by 5-30 amino acids that increases the drug translocation across cell membrane (18,19). The internalization of NPs can be made by direct diffusion, but the most common mechanism is based on endocytosis (**Figure 2. 3**) (28). Besides the specific targeting, the NPs present other advantages, such as protect the drugs from degradation, increase the drug delivery to tumor cells and modulate the pharmacokinetic profiles of the drugs, for example (13).

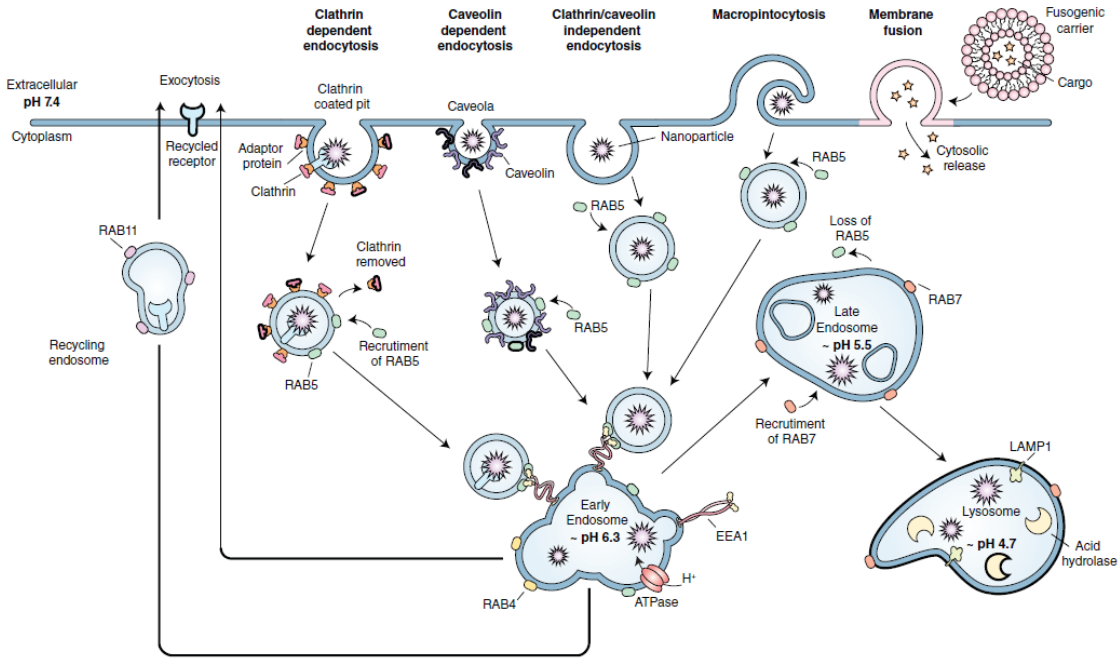

Figure 2. 3 - Mechanisms through which NPs can enter into target cells (28)

Due to their great biocompatibility, biodegradability and non-toxicity, PNPs are the most studied particles. Their properties depend on the type of polymers used, which can be synthetic or natural (13).

2.1.1. Types of Nanoparticles

There are several types of NPs, that are useful for cancer therapy (**Table 2. 1**), due to their ability of passive and active targeting of cancer cells, improvement of pharmacokinetic properties of the drugs and reversion of the mechanism of drug resistance (*e.g.*, by silencing drug resistance genes or proteins, like H1F1α and Bcl-2) (29). Therefore, NPs can offer many advantages such as selective drug accumulation in tumor sites, reduced amount of drug used and lower side effects (30). The main types of NPs used in cancer therapy are the polymeric NPs, the vesicle-based carriers (such as liposomes, micelles and dendrimers), the polymer-conjugates, the protein carriers, the inorganic NPs (such as metallic NPs) and the biologically-delivery NPs. However, the PNPs will be highlighted in this monograph (30).

Table 2. 1 - Most common NPs used in cancer therapy (29)

Nanocarriers	Properties	Characteristics
Solid Lipid NPs	Release drug in acidic microenvironment of multidrug resistance cells	Delivers anticancer drugs to overcome P-gp mediated multidrug resistance
PNPs	Versatile platform for controlled, sustained, and targeted delivery of anticancer agents including small molecular weight drugs and macromolecules (genes and proteins)	Enhanced drug accumulation, reduction of tumor size/volume, increased animal survival rate in rat models, minimal cytotoxicity in cancer cell lines, high transfection activity, potential to overcome multidrug resistance
Liposomes	Composed of lipid bilayers encapsulating both hydrophobic and hydrophilic drugs, stealth liposomes are surface coated with PEG	Long-circulating, prevents non-specific interactions, preferential accumulation in tumor tissues via enhanced permeability, and retention effect to overcome drug resistance
Micelles	Small size, high payload capacity, greater solubilization potential for hydrophobic drugs, improved stability, long circulation	Selective targeting, P-gp inhibitory action, altered drug internalization, and sub-cellular localization properties
Mesoporous silica NPs	Inorganic nanocarriers with tunable size and shape, high drug loading due to high pore volume and surface area, multifunctionalization for targeted, and controlled delivery	Enhanced cellular uptake and bioavailability, circumvents unwanted biological interactions, delivers therapeutics at cellular levels for therapeutic, and imaging in cancer

Inorganic NPs		
Iron Oxide Magnetic NPs	Unique optical, electrical, magnetic and/or electrochemical properties, inert, stable, ease of functionalization	Circumvents drug resistance associated with over expression of ATP-binding cassette transporters, increased intracellular drug retention, enhanced loss of cell viability
Gold NPs	Shape and size dependent on electronic characteristics, versatile drug delivery system due to tunable optical properties	Induces cellular DNA damage
Quantum dots	Semiconductor inorganic fluorescent nanocrystals, small (1–20 nm), and uniform size, high surface to volume ratio, surface conjugation with multiple ligands, biocompatible, fluorescence properties help real time tracks within target cells	Release of toxic compounds (cadmium) and generation of reactive oxygen species can result in long term toxicity

Generaly, PNPs present sizes ranging from 10 to 1000 nm and can be made of biocompatible and biodegradable polymers (31) that are flexible, lightweight, and non-toxic to the human body, such as chitosan, gelatin or albumin. These NPs have therapeutic potential as drug delivery systems, and therefore, for cancer therapy. The drugs can be entrapped, encapsulated or attached to the NPs (31,32). The main advantages reside on the increase of the stability, efficiency and effectiveness of the drugs used, and the possibility to deliver higher concentrations of therapeutic compounds to the desired location, allowing the application of PNPs in fields such as vaccine delivery or tissue engineering (31). Furthermore, PNPs are superior to lipidic NPs, such as liposomes, due to the higher compatibility with various active agents and loading volume, a more controlled drug release and the nonexistence of phospholipids oxidation (33).

One of the most common methods to produce PNPs is the dialysis or solvent exchange method. This method is surfactant free and allows the production of small and well distributed NPs. The polymer is dissolved in an organic solvent and placed into the dialysis membrane with proper molecular weight cut off. The solvent displacement leads to the polymer aggregation due to lower solubility and therefore to the formation of NPs (32). In **Figure 2. 4**, other methods for the preparation of PNPs are referred, including solvent evaporation, freeze and spray drying, fast evaporation, micro and mini emulsion, surfactant-free emulsion and controlled radical (32).

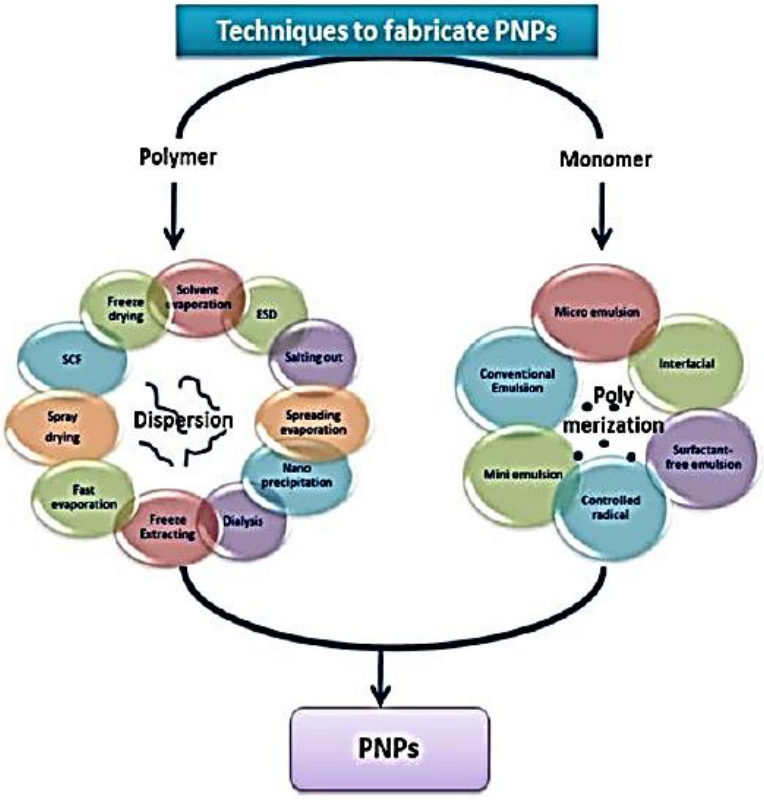

Figure 2. 4 - Several techniques to produce Polymeric NPs (32)

2.1.2. Main uses of Nanotechnology in Medicine

Despite its uses in electronics, transportation and energy,, NT is mostly known by its application in the medicine field, such as in neurodegenerative, inflammatory, cardiovascular and cancer diseases. Moreover, NT can combine the delivery of drugs and imaging agents in the nanosystems (34) for theranostic purposes (35).

2.1.2.1. Nanoparticles as Delivery Systems

The most promising application of nanomaterials is the possibility to specifically target their content, delivering small drugs as well as macromolecules such as proteins, peptides or genes, with few side effects (36,37). This specific delivery is possible due to the modification or functionalization of the NPs (37).

The different types of NPs can also be used for distinct applications (37). For example, metallic NPs can be linked to a fluorescent marker for drug delivery and imaging in magnetic resonance (37,38). Liposomes are also used in drug delivery, with the advantages of low cost production, wide range of morphologies and capability to encapsulate many types of therapeutic biomolecules (38). For example, cationic liposomal systems can transport charged structures such as DNA and RNA, due to the electrostatic interactions between the positively charged phospholipids and the negatively charged nucleic acids (39) . However, colloidal particles such as PNPs have attracted an increasing attention, in which a therapeutic agent can be embedded or encapsulated in their matrix or adsorbed or conjugated on their surface. Thus, PNPs are great carriers for biomolecules, drugs, genes and vaccines. However, they present some disadvantages, including short circulating life, being rapidly cleared by phagocytic cells (36) . This can be improved by modifying the NPs surface, for example by adsorbing PEG onto NPs surface. This increases nanoparticle blood circulation half-life, since the addition of PEG causes steric repulsion by creating hydrated barriers on nanoparticle surfaces, preventing their opsonization (36). Other hydrophilic polymers can be also used, such as polysorbates 80 and 20, poloxamers and polysaccharides, like dextran, that provide a cloud of hydrophilic and neutral chains at the NPs surface, repelling plasma proteins (36).

2.1.2.2. Nanoparticles for Biomedical Imaging

Several NPs are used for imaging purposes (**Table 2. 2**). For example, quantum dots, which are NPs constituted by inorganic semiconductor molecules, can emit florescence that depends on particle size, because of the movement of an electron from the conduction band to the valence band (band gap) when the excitation ends, leading to a release of energy (34). Also, superparamagnetic iron oxide NPs can be used in MRI as contrast agents (34,40). These NPs have a core made of iron oxide, usually with a hydrophilic coat, showing superparamagnetic behaviour that allows them to become

magnetized when a magnetic field is applied (40). Several studies have been applying these NPs to prostate cancer treatment, for example (40).

Table 2. 2 - Types of NPs used in biomedical imaging, their applications and characteristics (34)

Area	NPs types	Major *in vivo* applications	Significant characterization
Optical Images	Quantum dots	Site-specific imaging *in-vivo*	• Imaging of lymph nodes, lung blood vessels, and tumors. • Greater intensity and resistance to photobleaching compared with conventional methods. • Site-specific targeting via surface functionalization. • Sub-cutaneous imaging without surgical incisions.
MRI	Superparamagnetic iron oxide NPs	Cancer Detection	• Enhanced contrast for imaging of liver, lymph nodes, and bone marrow. • Paramagnetic properties that can alter magnetic resonance relaxation times of selected regions of fluids *in vivo*.

2.1.2.3. Nanomedicines for Theranostic Applications

Theranostic relies on the possibility to simultaneously diagnose and treat a disease (**Figure 2. 5-A**), being possible to real-time monitor the progress and efficacy of the treatment, thus allowing an individualized treatment and feedback (41). There are many types of theranostic carriers, such as gold, silver and magnetic NPs, nanoshells and nanocages, which can be functionalized with drugs, ligands or antibodies. The use of NPs can be combined with several noninvasive imaging methods, including MRI, computed topography, positron emission tomography/Computed Tomography (PET/CT), among others. (**Figure 2. 5-B**) (35,41).

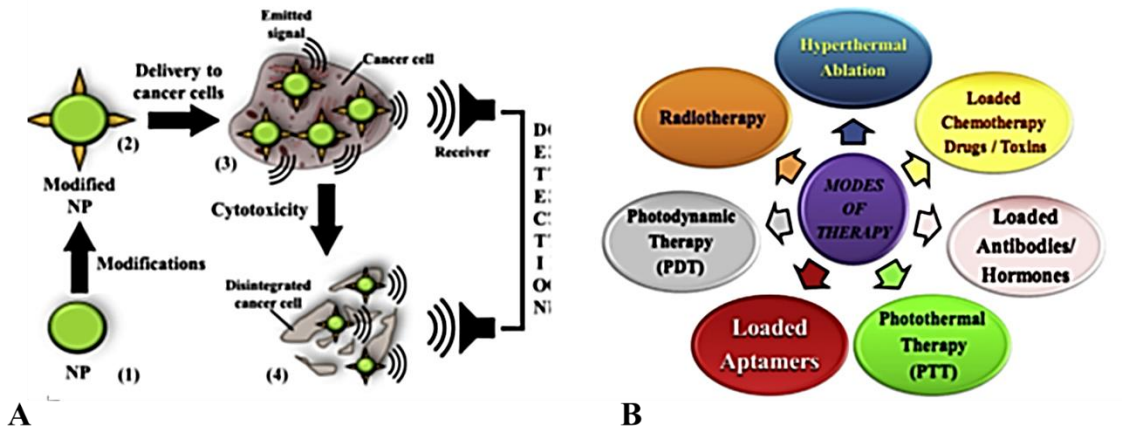

Figure 2. 5 - Nanotheragnostics: A- Scheme of a nanotheranostic agent; B- Approaches of nanotheranostic in cancer therapy (35)

2.2. Cancer: Actuality and Future Perspectives

Cancer is a disease in which the cells start to grow and spread uncontrollably, invading other organs and ultimately leading to the patient death (18). The stages in cancer progression are classified according to the size and extension of the tumor size and its ability to invade the nearby lymph nodes and/or other organs (18). The conventional treatment methods include surgery, radiation and chemotherapy. However, the chemotherapeutic agents target both normal and tumor cells due to the lack of specificity. In order to overcome this limitation, NT can be used as a strategy to target the drug delivery and minimize its side effects, by using ligands that target the overexpressed transporters and receptors on cancer cell membrane (18,19).

2.2.1. Cancer Epidemiology: Incidence, Mortality, Prevalence and Future Goals

Cancer is one of the diseases with highest incidence worldwide, with 14.1 million new cases in 2012 (15). Lung, breast, colorectal and stomach cancers comprise more than 40% of the total number of new cases. In men, lung and prostate cancer are the most common, whereas the breast cancer is the most incident in women (**Figure 2. 6**). Additionally, cancer caused 8.2 million deaths in 2012, more than half due to lung, stomach, liver, colorectal and breast cancers. Among the 32.5 million people diagnosed with cancer between 2007 and 2012, 6.3 million women had breast cancer, 3.9 million

men had prostate cancer, and the colorectal cancer was diagnosed in 3.5 million men and women (15–17).

In addition to all these numbers, the burden of cancer is expected to increase to 23.6 million new cancer cases per year by 2030, which represents an increase of 68% compared with 2012 (15).

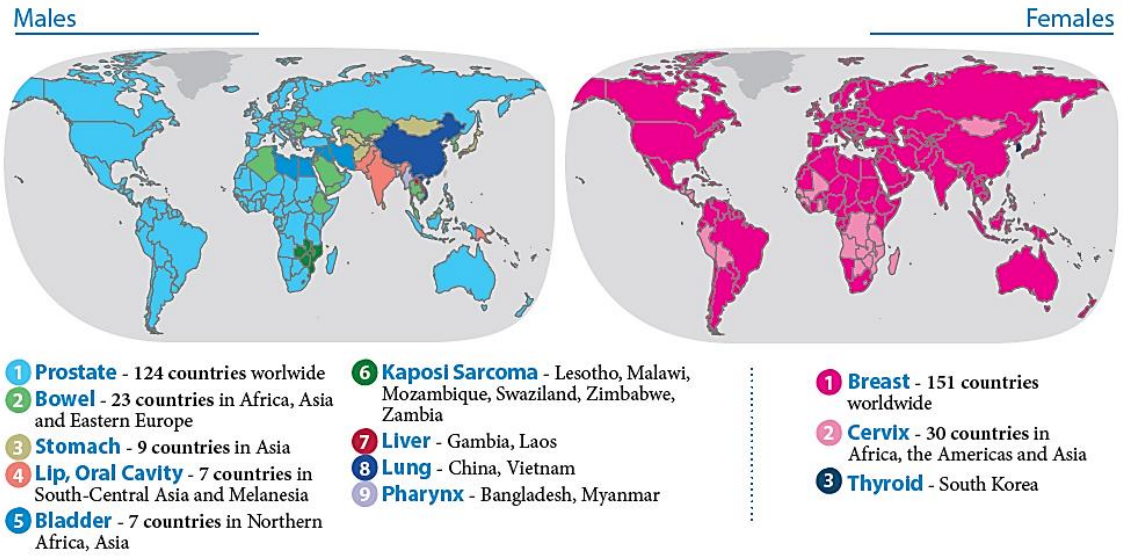

Figure 2. 6 - Most prevalent types of cancers by country, for males and females (15)

2.2.2. Cancer Therapies: Actual and New Perspectives

For almost all cancers, the main therapies include surgery, radiation and chemotherapy. However, due to their lack of specificity and effectivity, several efforts are being made to find new therapeutic solutions, mainly in the field of specific targeting therapy (18,19).

2.2.2.1. Breast Cancer

Breast cancer is the most frequent and lethal cancer in women (42). The diagnostic methods include mammography, MRI, ultrasound and PET/CT (42).The main modalities for breast cancer treatment include surgery, radiation therapy, chemotherapy and targeted therapy. Surgery is normally used in localized breast cancer and it is accompanied by neoadjuvant/adjuvant therapy to ensure fully recovery and decrease the risk of metastasis. Radiotherapy, a process in which radiation is applied to the cancer cells, can be combined with chemotherapy after surgery. Additionally, endocrine therapy can also be

systemically administered in order to lower the hormone levels or block the hormone receptors expressed on the cancer cells. However, systemic therapies (*e.g.*, chemo and endocrine therapies) can often cause side effects, such as hair loss, gastrointestinal disturbances, neutropenia, and immunosuppression, with a negative impact in the patients' quality of life. These problems led to several efforts aiming for the development of alternative treatments such as targeted drug delivery systems. These drug delivery systems showed to overcome the systemic toxicity and poor bioavailability problems associated with the antineoplastic drugs (43). The NPs can be used as contrast agents for imaging purposes, as drug carriers, as radiosensitizers or by inducing hyperthermia, causing apoptosis in the malignant tissues (42).

2.2.2.2. Prostate Cancer

Currently, prostate cancer is diagnosed in more than 1 million men per year worldwide and it was responsible for 307.000 deaths in 2012 (44). The diagnosis of prostate cancer can be done by screening of prostate-specific antigen (PSA) levels. PSA is an enzyme produced only by prostate cells, but it is not specific for prostate cancer, because the PSA levels can also be elevated in other pathologies, such as prostatitis, prostate abscess and prostatic infection (45). The main types of treatment are prostatectomy (removal of prostate), radiotherapy, brachytherapy (insertion of a radioactive source directly into the prostate) and hormone therapy (first option for non-metastatic tumors) (44,45). However, most of these treatments can cause side effects or lead to cancer recurrence and resistance to the posterior treatments (44). Thus, the use of drug carriers, particularly liposome, PNPs and metallic NPs, have been investigated in order to overcome these limitations (44).

2.2.2.3. Colorectal Cancer

Colorectal cancer is the third most commonly diagnosed type of cancer with 20–25% of the patients presenting metastasis at the time of diagnosis, usually done by colonoscopy (46). Because of that, most of the patients have palliative treatment instead of curative, since the neoplasm is already in an advanced stage when it is diagnosed (46,47). Several systemic drugs have been used for the treatment of colorectal cancer, such as 5-fluorouracil, irinotecan, oxaliplatin and some monoclonal antibodies

(bevacizumab, cetuximab and panitumumab) and their combination have shown some improvement in the treatment. The guidelines also recommend surgery, immunotherapy and radiotherapy, all of them possible to be used in combination (46). Additionally, NPs have been studied for diagnosis and treatment purposes, using nanobioconjugates as contrast agents (*e.g.*, tunable quantum dots) for fluorescence-based imaging techniques, as well as, through the use of NPs (*e.g.*, gold NPs) to specifically deliver cytotoxic drugs into cancer cells, increasing their effectiveness and reducing the side effects (47,48).

2.2.3. Use of Nanomedicines in Cancer Therapy

NT is an emerging tool in cancer therapy through the use of nanobioconjugates composed by NPs and specific molecules for diagnostic or therapeutic purposes, such as contrast agents, chemotherapeutic drugs and targeting ligands. The stability of nanobioconjugates in blood can vary from hours to days, depending on the surface proteins, which can prevent the aggregation or agglomeration process, protecting them. As already mentioned, these nanobioconjugates can act by passive and/or active targeting (**Figure 2. 7**) (47,49). The passive targeting occurs due to the bigger fenestrations between the endothelial cells that surround the cancer cells than the normal cells, so called EPR effect., which allows the extravasation of NPs with sizes between 100 to 600 nm and their accumulation in the tumor tissue (47,50). Also, due to the high metabolism exhibited by cancer cells, the environment around them is more acidic than in normal cells, which allows the degradation of pH-sensitive NPs (stable at a physiologic pH), releasing active drug only in acidic environments, such as in tumor cells (20). However, the active targeting can effectively deliver the payloads to the cancer cells, in which the nanocarriers functionalized with antibodies, peptides and nucleic acids can specifically bind to the receptors in the surface of target cells (47). This targeted delivery of drugs through nanobioconjugates leads to a decreased toxicity of the drug in normal tissues as well as a reduced multidrug resistance (50). For example, studies shown that NPs may solve the problem of *P*-glycoprotein (*P*-gp) related multi-drug resistance (51,52), since the drug molecules associated with a nanocarrier would be released slowly in cancer cells, avoiding the activation of drug resistance-related genes. Also, NPs are considered a poor substrate for *P*-gp, allowing drugs to remain inside the cells, where their anti-cancer activities are most effective (53). Others strategies studied were the use of NPs containing

a siRNA-mediated silencing of *P*-gp (54) or the use of the copolymer Eudragit, specially Eudragit S100, as excipient for NPs preparation (52).

Because of such properties, nanobioconjugates can be used for diagnostic or treatment purposes or combine both modalities for theranostic applications (35).

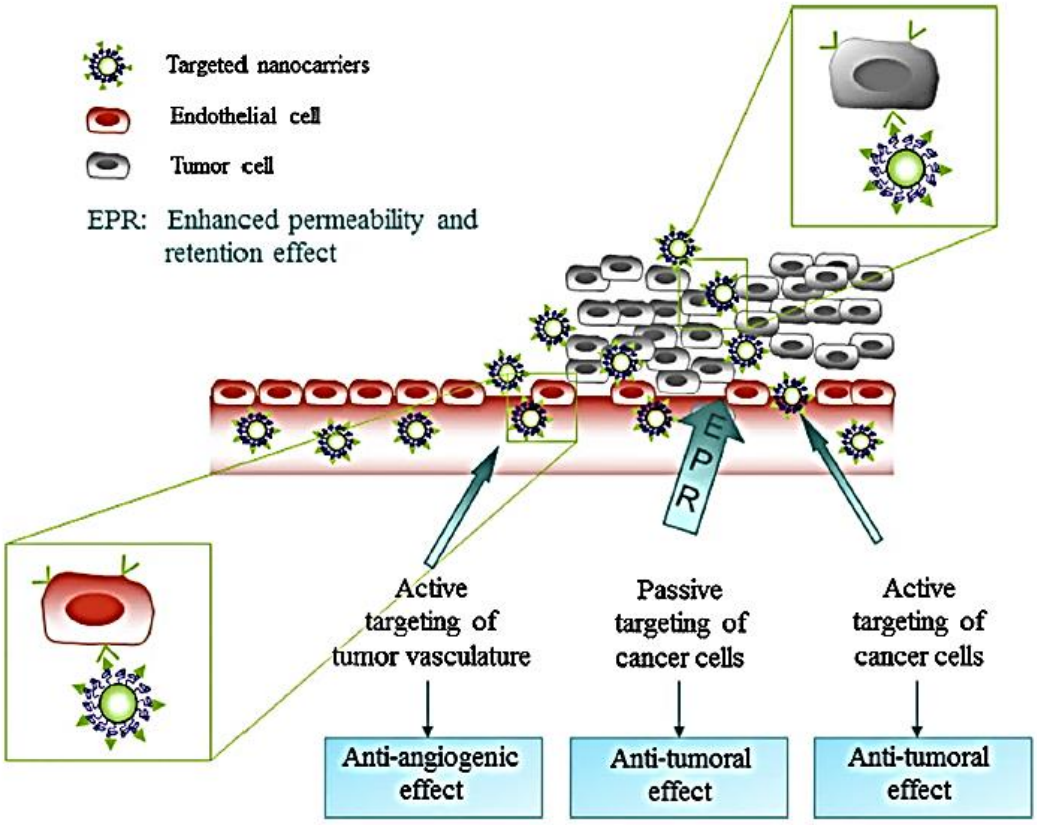

Figure 2. 7 – Schematic representation of the passive and active targeting (49)

2.2.3.1. Use of Polymeric Nanoparticles in Cancer Therapy

PNPs are colloidal particles in which an anticancer agent can either be encapsulated within their polymeric core or adsorbed, or conjugated onto NPs surface (22). For their formulation, hydrophilic, non-toxic and biocompatible polymers can be used, such as polyvinyl alcohol and PEG. Furthermore, PEGylation can prevent the process of phagocytosis and opsonisation by providing a hydrophilic coating on the NPs' surface (22). Thus, the anticancer can be localized within the hydrophobic core of the NPs surrounded by a hydrophilic shell, increasing their systemic circulation time, and thereby, their persistence in the bloodstream. Several ligands can be used to functionalize the NPs, including small molecules, peptide, proteins, antibodies, engineered antibody fragments,

and aptamers, that target specific receptors expressed on the membrane of cancer cells and/or endothelial cells present in the tumor vasculature (22). For example, folate receptors, epidermal growth factor receptors and the transferrin receptors are mostly present on cancer cells, while integrins, vascular cell adhesion molecule-1, aminopeptidase N/CD13, membrane type 1 matrix metalloproteinase and vascular endothelial growth factor receptors, are mostly expressed on the vasculature of tumor cells (22,55).

Other polymers have been investigated as delivery vectors of chemotherapeutics into cancer cells, including polypeptides (*e.g.*, poly (L-lysine)), natural (*e.g.*, chitosan, dextran and hyaluronic acid, for example) and synthetic (*e.g.*, polyamidoamine) polymers (55). In fact, PNPs tend to accumulate in specific organs. For example, dextran sulphate binds to more receptors on liver sinusoidal endothelial cells than hyaluronic acid and thus it accumulates more in the liver (56). Other example are NPs coated with anionic poly (glutamic acid)-based peptides that show tissue-specificity to spleen and bone (57).

2.3. Lignin as a Starting Biomaterial for an End-use Applications

The term lignin derives from Latin word *lignum*, which means wood (24). Lignin is one of the three components of lignocellulosic biomass, along with cellulose and hemicellulose. Lignin is the second most abundant natural substance in nature after cellulose, (24,58) and an abundant renewable source of aromatic polymers on earth. Lignin has been studied for 30 years because of its attractive characteristics such as high content in aromatic structure, wide availability and potential to be modified (59). However, lignin is a challenging starting material to work with due to its characteristics, such as complex macromolecular structure that depends on its botanic origin, isolation procedure and high molecular heterogeneity within the same batch (59). Despite of these challenges, several high-value products obtained from lignin have been produced, such as vanillin, dimethyl sulfoxide, active carbon and carbon fibers (58) . According to that, lignin has been used for end-use applications, which are summarized in **Figure 2. 8** (58).

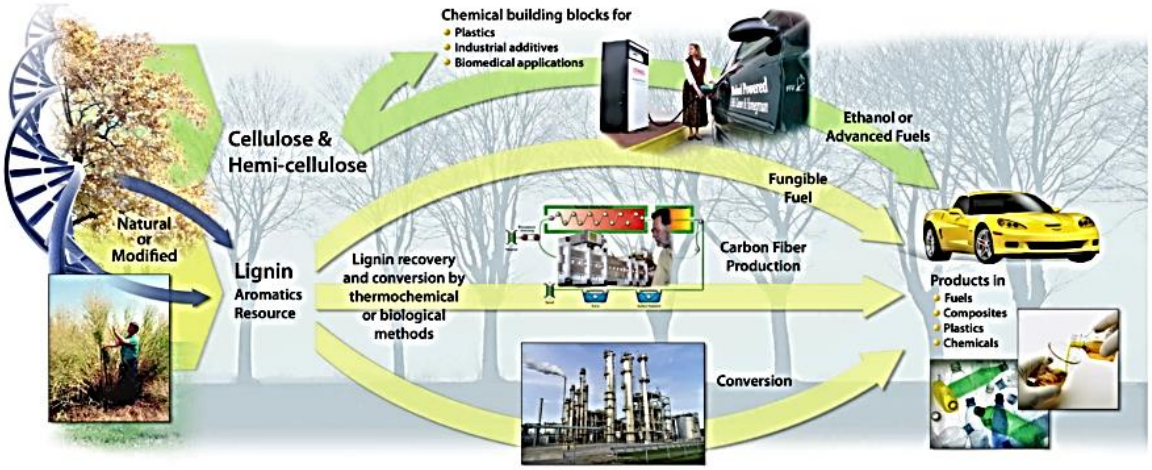

Figure 2. 8 - Several end-use applications of lignin (58)

2.3.1. Biologic Origin and Degradation of Lignin

From an evolutionary point of view, the presence of lignin in the plant structure enables the development of the tracheid cell type, permitting a better transportation of water in the plant and the expansion of plants into dryer land (60). So, the fraction of lignin varies according to the different sources of biomass. The highest lignin fraction is typically found in softwood which ranges between 25 and 32 wt%, while in hardwoods is slightly lower (18–25%) (60). For grass is even lower, and it is almost absent in mosses and green algae, which reflects the major milestones of evolution of lignin biosynthesis (**Figure 2. 9**) (60,61).

Lignin is typically composed by three different monomers called monolignols: *p*-coumaryl, coniferyl and sinapyl alcohols. When incorporated into the lignin structure, these monolignols originate units that are commonly referred as hydroxyphenyl (H), guaiacyl (G) and syringyl (S) units, respectively (61).

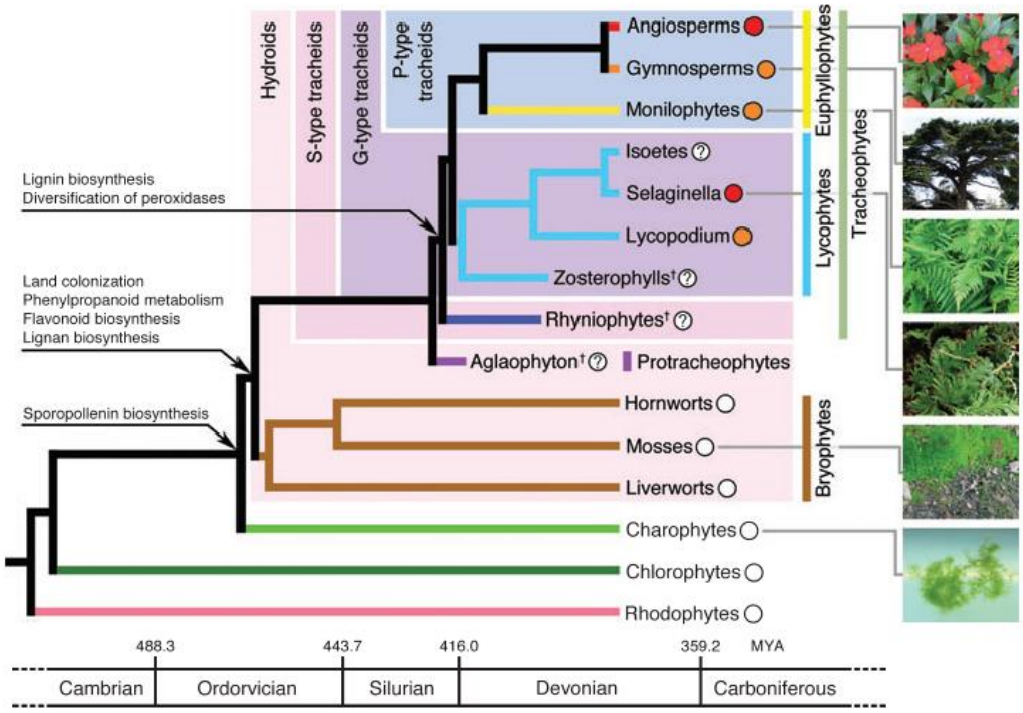

Figure 2. 9 - Evolution of lignin biosynthesis represented by a plant phylogenetic tree (61)

The initial step for the biosynthesis of the lignin building blocks is the formation of cinnamic acid from phenylalanine, through the action of the enzyme phenylalanine-ammonia-lyase. Cinnamic acid is then converted into the three basic monolignols and after to the respective units through several reactions (60), including dehydrogenations, reductions, hydroxylases and transference of several chemical groups, such as methyl groups (**Figure 2. 10**) (61). Afterwards, the polymer is formed after enzymatically catalysed oxidation of the phenol groups of the monolignols, which originates monolignol radicals that polymerize into the basic building blocks of the lignin polymer (60). The relative proportions of the building blocks vary depending on the type of biomass. For example, the guaiacyl unit is dominant in softwoods (90–95%), but the amount of syringyl units (45–75%) is bigger than the guaiacyl units in hardwoods. Lignin in grasses contains significant amount of *p*-hydroxyphenyl units (5–35%), which is practically absent in both softwoods and hardwoods (60).

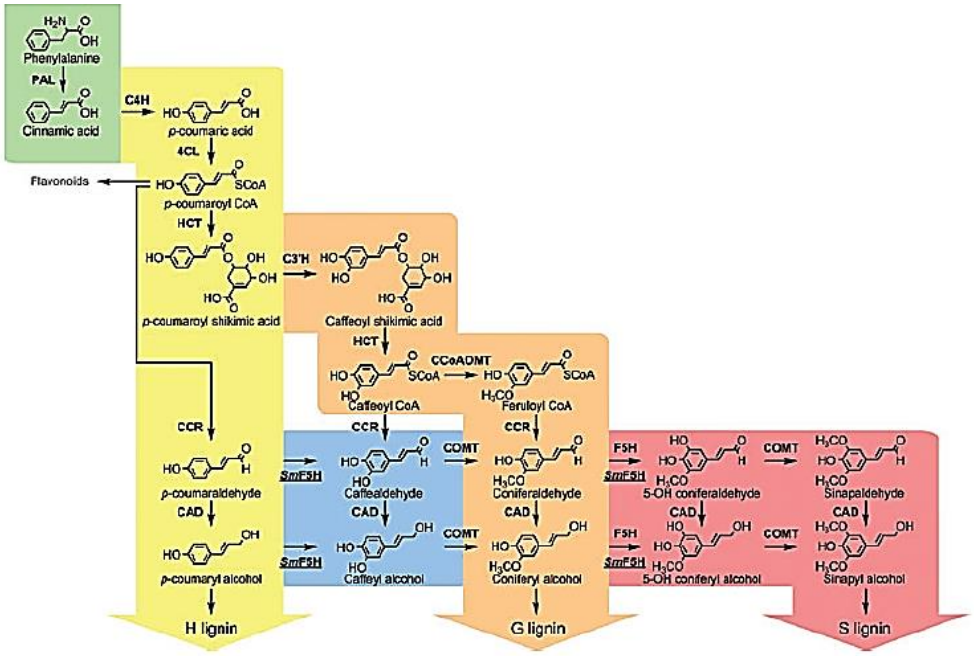

Figure 2. 10 - Synthesis of the different types of units present in the lignin structure (61)

2.3.2. Structure and Characterization of Lignin

As above mentioned, the lignin monomers are called monolignols and consist of phenylpropanolic units that present different degrees of substitution of the methoxy groups on the aromatic ring, as shown in **Figure 2. 11** (59).

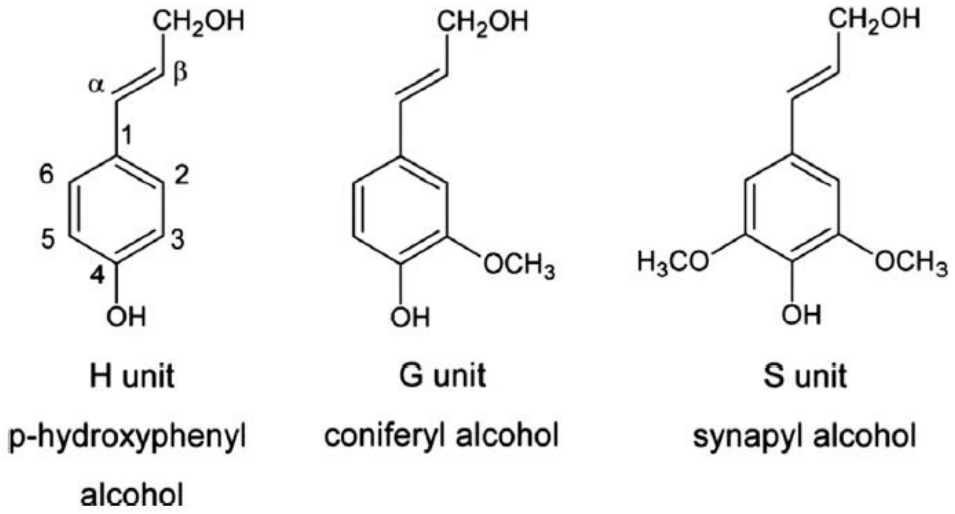

Figure 2. 11 - The monolignol monomers species present in the lignin structure (59).

The primary structure of lignin is formed by radical polymerization of monolignols by peroxidases and lactases that lead to the formation of an important variety of inter-unit linkages. The *β*-O-4' ether linkages are the most abundant and involve the binding of the *β* carbon of one unit with the phenolic hydroxyl group of the other unit. Other linkages include α-O-4' ether and 4-O-5' diphenyl ether, for example (59,60). According to this, the proportions of the three monomer types in lignin influences the type of inter-unit linkages, which also determines the degree of branching and the reactivity of lignin (59,60).

However, the structure of lignin in nature is different from the lignin obtained as a co-product in the industrial cooking process, used to solubilize the nature lignin, insoluble in water, and thereby separate it from the fiber fraction, forming technical lignin (60). Its structure is also dependent on the cooking method applied (60). Therefore, the proportion of the different linkages present in technical lignins will be different from those existing in the native lignin (60). Technical lignins are divided into two categories, according to their sulfur content. The first one includes the sulphur-containing commercial lignins, such as lignosulfonates and kraft lignins, which can be produced in large quantities. The second one includes lignins without sulphur in their composition, such as organosolv and soda lignin (62). These lignin can be further used as a substrate for chemical functionalization in order to produce high value products (59).

2.3.3. Valorisation and renewal of Lignin

Lignins and their derivatives have been included in many pharmacological studies (**Table 2. 3**), which showed their potential for the treatment of diabetes and emphysema, to control obesity, as well as used as anticoagulant, (23), antiviral, antioxidant, prebiotic and antibiotic (23,58). In addition, natural lignin is considered to be part of dietary fiber resistant to digestion. (58).

Table 2. 3 - Main pharmacological activities of lignins and their derivatives (23)

Compound	Effect	Mechanism	Experimental Model
Alkali lignin	Antidiabetic	α-amylase inhibition *In vitro* decreased glucose diffusion	*In vitro* glucose movement
Lignosulfonic acid	Antidiabetic	Inhibitor of α-glucosidase Decrease blood glycemia	*In vitro* inhibitor of α-glucosidase Rat *in vivo*
	Antiviral activity	Inhibition of the replication of herpes simplex virus (HSV)	Infected mice by exposing scarified skin to an HSV-2 G
		Binding to the HIV-1 envelope glycoprotein	*In vitro* cells: T-lymphoma cell lines, HEK293T, HUT-78, Monocyte-derived dendritic cells
Lignin–carbohydrate complexes	Antiviral activity	Inhibiting viral binding and penetration	Vero cells infected with herpes simplex virus
		Binding the HIV-1 envelope glycoprotein	HeLa cells infected with herpes simplex virus
Lignophenols	Obesity control	Decrease oleate-induced apo-B secretion	HepG2 cells *in vitro*
		Decrease plasma triglyceride levels	Rats fed a high-fat diet
Sulfated low molecular-weight lignins	Anticoagulant	Inhibition of thrombin	Binding to thrombin
		Allosteric inhibition of thrombin	Whole blood thromboelastography, hemostasis analysis and mouse arterial thrombosis models
	Antiemphysema	Elastase, oxidation and inflammation inhibition	*In vitro* human alveolar A549 and bronchial Calu-3 epithelial cells

However, lignin valorization is also applied in biorefinery processes (63,64). Currently, most lignocellulosic biorefineries use enzymes to decompose plant polysaccharides to produce lignin-rich streams by separating the lignin in the solid state from the others plant carbohydrates or by applying pretreatments to fractionate biomass to extract lignin (63). The pretreatments of biomass can consist on using dilute sulfuric or other acids, or simply hot water (hydrothermal) to break down hemicellulose to sugars and to increase cellulose accessibility for enzymatic hydrolysis, after which most of the lignin is left in the solid residue. In other pretreatment methods, high pH conditions are applied to dissolve a large portion of the lignin (63). Other treatments consist of using microbial conversion, using specific microbes to catalyze the degradation of a heterogeneous mix of aromatic molecules to single products, such as lignin (64).

After extraction of lignin, this compound can be used in several industrial applications. For example, lignin products have been studied to be a platform for the global development of energy-efficient lightweight vehicles, since lignin has become an ideal precursor for carbon fiber synthesis, using different types of reactions, such as oxidations or pyrolysis, as described in **Figure 2. 12** (63).

Another lignin application is for the production of plastics and composites (63). For example, formulations either without chemical modification of lignin, including phenol-formaldehyde resins, polyolefin, polyester polymers, polyurethanes and bio-plastics, or with chemical modifications, such as lignin-based epoxy resins for wood adhesion, have been used to produce different materials, including mineral wool; stabilized materials against photo-oxidative degradation, as well as other ecofriendly products (58). Lignin have also been studied to produce other high-value materials than carbon fiber, such as vanillin, dimethyl sulfoxide and active carbon (63).

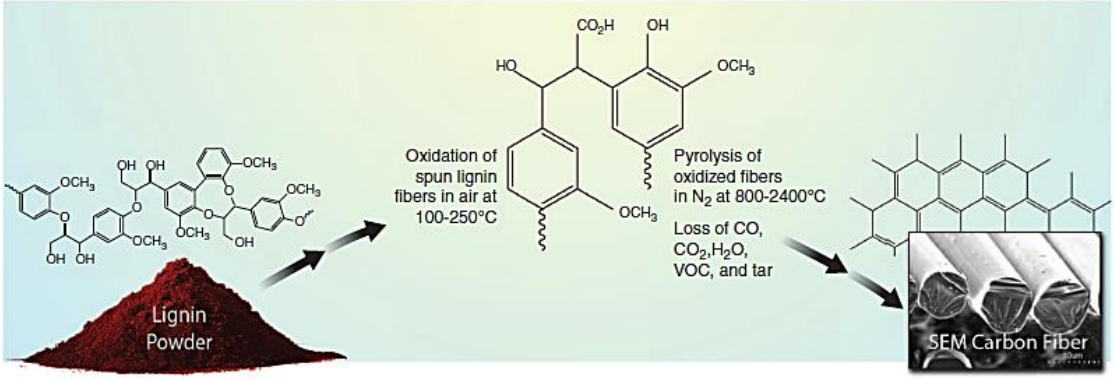

Figure 2. 12 - Thermal treatment applied to convert lignin into carbon fibers (63)

2.3.4. Chemical Modifications of Lignin

Lignin is a very good candidate for the development of new materials due to the presence of phenolic and aliphatic hydroxyl groups in its structure (23). For example, phenolic hydroxyl groups and aliphatic groups at C-α and C-γ positions enable the lignin utilization as a substitute for phenol in the synthesis of phenolic resins, for example (65). Other chemical modifications involving the reactivity of hydroxyl groups on the natural polymer are esterification and etherification reactions. In addition, the introduction of reactive amine groups in the lignin has been considered as one of the most promising processes, since the aminated lignin can be employed in the preparation of polyurethane or epoxy resins. (66).

The epoxidation of lignin has also been gaining importance for the production of epoxy resins, which can be used for adhesives, composites and coatings (62).

Other type of chemical modification of lignin is the carboxylation (67), which will be used in this project before the preparation of the NPs.

2.3.5. Preparation of Lignin Nanoparticles

According to the extraction methods, there are different types of lignins, such as kraft lignin, soda lignin, lignosulphonate and organosolv lignins (68,69), as represented in **Figure 2. 13**.

Although each lignin class has a specific chemical structure and particular properties, lignin possesses unique properties such as resistance to biological attacks, UV absorbance, high stiffness, and antioxidative properties, showing promising potential to produce high value products, including NPs. At the same time, most lignins are only soluble in water at alkaline pH, which is a major limitation for its application at an industrial scale (69). Despite of this, lignin has been shown potential for preparing LNPs (69).

Lignin is indeed one of the most abundant biopolymers in nature, being biodegradable, biocompatible and it presents very good stability, which makes it an ideal precursor for the development of environmentally friendly nanomaterials, suitable for being used as stabilizers in cosmetic and pharmaceutical formulations and for drug delivery of anticancer compounds (23,25). Also, innovative LNPs have shown others

features, important for drug delivery and biomedical applications, such as the ability to carry hydrophobic drugs and sustain their release, as well as good cellular interactions (23,25). As a result of their surface structure, LNPs can also be modified with targeting molecules in order to increase cellular interaction with specific cells for cancer therapy, for example. Also, pH-sensitive polymers can be added to the LNPs to allow pH-responsive drug release (23,25).

A

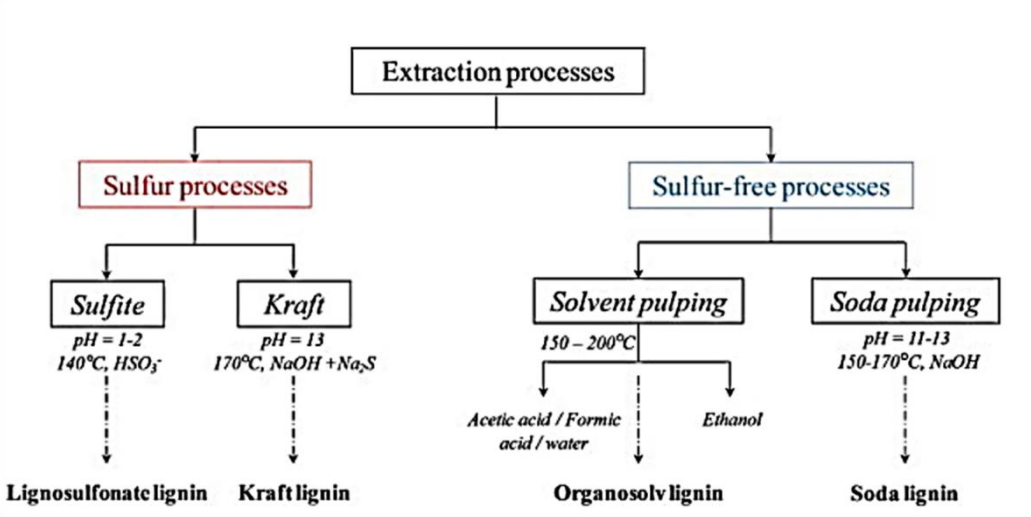

B

Lignin type	Sulfur-lignins		Sulfur-free lignins	
	Kraft	Lignosulfonate	Soda	Organosolv
Aspect				
Raw materials	Softwood Hardwood	Softwood Hardwood	Annual plants	Softwood Hardwood Annual plants
Solubility	Alkali Organic solvents	Water	Alkali	Wide range of organic solvents
Number-average molar mass (M_n – g mol^{-1})	1000–3000	15,000–50,000	800–3000	500–5000
Polydispersity	2.5–3.5	6–8	2.5–3.5	1.5–2.5
T_g (°C)	140–150	130	140	90–110

Figure 2. 13 - General characteristics of the different types of lignin: A) extraction processes of each type of lignin; B) Physical and chemical characteristics of each type of lignin (68)

2.3.5.1. Preparation Methods of Lignin Nanoparticles

LNPs have been previously synthesized using several methods, including solvent exchange (that can produce both solid and hollow particles), antisolvent precipitation, sonication, polymerization, interfacial crosslinking, aerosol processing and CO_2 precipitation (69). In the antisolvent precipitation method, the precipitation of the solute is achieved by decreasing the solvent power for the solute dissolved in a solution, adding a non-solvent for solute called as antisolvent (70).

For example, the solvent exchange method is often performed by dialysis and antisolvent precipitation method are initiated with acids (71). Initially, exchange method was done by dialysis using ethylene glycol as a solvent, which resulted into irregular NPs (72). However, other studies have shown the possibility of preparing NPs, like LNPs, with an acceptable average diameter, prepared from soft wood kraf lignin dissolved in tetrahydrofuran (THF), introduced into a dialysis bag immersed in excess of deionized water during 24 hours (25,72).

The physical properties of these particles such as hydrophobicity, surface charge, and stability are dependent on the type of lignin used and the nanoparticle preparation method (71).

2.3.5.2. Delivery Systems for Biomedical Applications

As already referred, LNPs exhibit important features for drug delivery and biomedical applications, such as the possibility for carrying hydrophobic drugs (such as BZL and sorafenib) (25). Another very important characteristic of these LNPs is the possibility for being modified by targeting molecules in order to increase the cellular uptake by specific cells (23,25). All these characteristics make lignin an ideal starting material for the development of environmentally friendly nanomaterials that can be used for anticancer therapy (25). For example, LNPs loaded with BZL and sorafenib showed inhibitory effects on different cancer cells including MDA-MB-231 and MCF-7 (human breast cancer cell lines), PC3-MM2 (a prostate cancer cell line), Caco-2 (colorectal adenocarcinoma) (25). These LNPs also showed a moderately uniform dispersity, biocompatibility, very good stability, good cellular interaction, a time and dose-dependent cellular uptake, an improvement of the release profiles of both drugs at different pH-values and an enhancement of the antiproliferative effect of BZL in different cell lines (25).

According to this study, LNPs showed potential as delivery systems for cancer therapy. In the future, the addition of pH-sensitive polymers to these LNPs can induce a pH-responsive release of drugs which is an important strategic to be studied for cancer therapy (25).

3. Aims of the study

Several studies have shown the potential of lignin as a polymer for NPs production, due to its abundance and biodegradable characteristics. Given the potential already demonstrated of LNPs for anticancer therapy, the main aim of this study was to evaluate the characteristics and potential CLNPs as a delivery system of anticancer compounds.

The specific objectives of this monography were as follow:

1. To synthetize carboxylated lignin, and therefore, prepare and characterize CLNPs.

2. To conjugate the CLNPs with the block copolymer PEG-PHIS and CPP in order to prepare CLNPs-CPP and CLNPs-PEG-PHIS-CPP, using 1-ethyl-3-(3-dimethylaminopropyl) carbodiimide hydrochloride and N-hydroxysuccinimide (EDC/NHS) coupling chemistry.

3. To characterize the prepared CLNPs by dynamic light scattering (DLS) and transmission electron microscopy (TEM), and to evaluate their stability in human plasma and cell culture media, as well as *in vitro* cytotoxicity in different cell lines: MDA-MB-231 (human breast cancer cell line), PC3-MM2 (a prostate cancer cell line), Caco-2 (colorectal adenocarcinoma) and EA.hy926 (a non-tumor endothelial cell line).

4. To evaluate the loading and release profiles of a poorly water-soluble cytotoxic compound, BZL, at different pH values (5.5 and 7.4).

5. To realize *in vitro* antiproliferative studies of the BZL-loaded CLNPs using the cell lines mentioned above.

4. Materials and Methods

4.1. Material and Cell Culturing

LignoBoost™ softwood kraft lignin was obtained from Stora Enso (Finland). BZL (8-isopropyl-1-methyl-4-(trifluoromethyl)-3H-benzo[cd]azulen-3-one) was synthetized as described elsewhere (73). CPP was purchased from GenicBio (China), α-t-butyloxycarbonylamino-ω-carboxy succinimidyl ester (Boc-NH-PEG-NHS; MW = 4928 Da) from Iris Biotech GmbH, and Poly(hystidine) (PHIS; MW = 14200 Da) from Sigma-Aldrich. Other materials and cell culturing are described in detail in **Supporting Information**.

4.2. Carboxylation of Lignin

Carboxylated lignin was prepared in order to increase the amount of carboxylic groups on the lignin structure for further conjugation reactions. For that, 100 mg of LignoBoost™ softwood kraft lignin was reacted with 100 mg of succinic anhydride and 20 mg of 4-dimethylaminopyridine (DMAP) in 40 mL of THF at room temperature for 48 h. Then, the reaction mixture was dialyzed against MilliQ-water using a dialysis bag (Spectra/Por® 1 Standard RC Dry Dialysis Tubing, 12-14 kDa, Spectrum Labs, USA) during 24 h to remove the unreacted reagents, replacing the water periodically. Finally, the carboxylated lignin was freeze-dried and characterized with a Fourier transformed infrared spectroscopy (FTIR) instrument (Vertex 70, Bruker, USA) using a horizontal attenuated total reflectance (ATR) accessory (MIRacle, PIKE Technologies, USA). The ATR-FTIR spectra were recorded at room temperature between 4000−650 cm^{-1} with a resolution of 4 cm^{-1} using OPUS 5.5 software.

4.3. Synthesis of Poly(Ethylene Glycol)-Block-Poly (ι-Histidine) (NH_2-PEG-PHIS)

The block copolymers were synthetized and characterized as previously reported (74)**.** Briefly, first the conjugation between Boc-NH-PEG-NHS and PHIS was made, and after, the deprotection of Boc-NH-PEG-PHIS was carried out (**Figure S1**). The detailed protocol can be found in **Supporting Information**.

4.4. Carboxylated Lignin Nanoparticles Preparation

The CLNPs were prepared by solvent exchange. Briefly, the carboxylated lignin was dissolved in THF and introduced into a dialysis bag (Spectra/Por® 1 Standard RC Dry Dialysis Tubing, 12-14 kDa, Spectrum Labs, USA). The CLNPs were formed during the dialysis process, where the THF soluble and water non-soluble carboxylated lignin molecules self-assembled into colloidal spheres as THF was gradually replaced by deionized water (72)**.** The dialysis water was periodically replaced during 24 h and the dialysis was performed under slow stirring in a fume hood.

4.5. Characterization of Carboxylated Lignin Nanoparticles

CLNPs were characterized for their average particle size (Z-average), polydispersity index (PDI), and average ζ-potential (surface charge) by DLS using a Malvern Zetasizer Nano ZS instrument (Malvern Instruments Ltd, UK). For that, the samples were diluted in MilliQ-water (100 µg/mL for the size determination and 10 µg/mL for the ζ-potential determination). To characterize their morphology and confirm their size distribution, the CLNPs were observed by TEM (TEM, Jeol JEM-1400, Jeol Ltd., Tokyo, Japan) using an acceleration voltage of 120 kV. For the sample preparation, a droplet of CLNPs' suspension was placed on a carbon-coated copper grid, blotted using a filter paper, and then air-dried before analysis.

The stability of CLNPs was assessed in Dulbecco's Modified Eagle medium (DMEM) and human plasma. For that, samples were withdrawn at 5, 10, 30, 90 and 120

min after incubation of 300 µg/mL of CLNPs with the different media at 37 °C, and diluted in water to evaluate changes on the size of CLNPs over time. All the experiments were performed in triplicates.

4.6. Conjugation of Carboxylated Lignin Nanoparticles with NH_2-PEG-PHIS and CPP

The conjugation reaction between the –COOH groups of carboxylated lignin and $–NH_2$ groups of NH_2-PEG-PHIS and CPP was performed in 10 mM of 2-(N-morpholino)ethanesulfonic acid (MES) buffer pH 5.5, using EDC/NHS coupling chemistry. The mass ratios of polymer/peptide for the conjugation reactions were chosen after optimization of the conjugation conditions. In order to prepare CLNPs conjugated with CPP (CLNPs-CPP), 1 mg of CLNPs was suspended in 400 µL of 10 mM of MES buffer (pH 5.5), with 2.5 µL of EDC (20 mM, MW = 155 Da) and 2.3 mg of NHS (50 mM, MW = 115 Da), and stirred at 500 rpm for 1 h at room temperature in the dark to activate the carboxylic groups on the CLNPs. Then, the mixture was centrifuged to remove the exceeding EDC/NHS, at 13200 rpm for 5 min, and the CLNPs were resuspended with 1 mL of 1× Hanks' balanced salt solution with 4-(2-hydroxyethyl)-1-piperazineethanesulfonic acid (HBSS-HEPES, pH 7.4) containing 0.2 mg of CPP (mass ratio CPP:CLNPs of 1:5). The mixture was stirred at 500 rpm and room temperature during 4 h and afterwards centrifuged to separate the functionalized CLNPs from the free CPP. Finally, the CLNPs-CPP were washed twice with HBSS-HEPES (pH 7.4).

For the preparation of the CLNPs conjugated with NH_2-PEG-PHIS and CPP (CLNPs-PEG-PHIS-CPP), 1 mg of CLNPs was activated for 1 h, using the same conditions as described above. After removing the exceeding EDC/NHS, the CLNPs were resuspended with 1 mL of 10 mM of MES buffer (pH 5.5) with 0.1 mg of NH_2-PEG-PHIS dissolved (mass ratio co-polymer: CLNPs of 1:10), and the mixture was reacted during 4 h at 500 rpm, and at room temperature. Then, the mixture was centrifuged to separate the functionalized CLNPs from the free co-polymer, and the CLNPs-PEG-PHIS were resuspended with 400 µL of HBSS-HEPES (pH 7.4), with 2.5 µL of EDC (20 mM, MW = 155 Da) and 2.3 mg of NHS (50 mM, MW = 115 Da). The mixture was stirred during 1 h at 500 rpm and at room temperature, in the dark to activate the carboxylic groups of the CLNPs-PEG-PHIS. After removing the unreacted products by

centrifugation, 1 mL of HBSS-HEPES (pH 7.4) containing 0.2 mg of CPP (mass ratio CPP:CLNPs-PEG-PHIS of 1:5) was added to CLNPs-PEG-PHIS, and the mixture was stirred for 4 h at 500 rpm and at room temperature. Lastly, the CLNPs-PEG-PHIS-CPP were centrifuged and washed twice with HBSS-HEPES (pH 7.4).

Besides the characterization by DLS, the functionalized CLNPs were also evaluated by ATR-FTIR.

4.7. Cell Viability Studies

Human umbilical vein cell line (EA.hy926), human mammary carcinoma cell lines (MDA-MB-231 and MCF-7), human prostate cancer cell line (PC3-MM2), and human colorectal adenocarcinoma cell line (Caco-2) were seeded in 96-well plates (PerkinElmer Inc., USA) at a density of 15000 cells per well and allowed to attach overnight. Afterwards, 100 µL of CLNPs, CLNPs-CPP and CLNPs-PEG-PHIS-CPP suspensions in cell media at different concentrations (50, 100, 250 and 500 µg/mL) were added to each well and the plates were incubated during 24 h at 37 °C. Incubations with cell media and 1% (v/v) Triton X-100 were used as a positive and negative controls, respectively. After that, the plates were equilibrated at room temperature for 30 min and the wells were washed once with 100 µL of HBSS–HEPES buffer. Then, 50 µL of Cell Titer-Glo® (Promega Corporation, USA) were added to 50 µL of HBSS–HEPES (pH 7.4) in each well. The plates were stirred for 2 min on an orbital shaker and then stabilized for 30 min at room temperature, protected from the light. Finally, the luminescence was measured using a Varioskan Flash plate reader (Thermo Fisher Scientific Inc., USA). The number of viable cells in culture was quantified based on the amount of ATP produced by metabolically active cells (25,75).

4.8. Loading of BZL

Here, a poorly water-soluble cytotoxic agent (BZL), was used as model to test the drug loading into CLNPs. For that, 2 mg/mL of carboxylated lignin dissolved in THF were mixed with 400 µg of BZL dissolved in THF (weight ratio drug:lignin of 1:5), and then introduced into a dialysis bag (Spectra/Por® 1 Standard RC Dry Dialysis Tubing, 12-14 kDa, Spectrum Labs, USA). The BZL-loaded CLNPs (BZL@CLNPs) were formed

during the dialysis process using MilliQ-water (periodically replaced), for at least 24 h in order to remove THF and free BZL.

The conjugation reactions of BZL@CLNPs with CPP and PEG-PHIS-CPP were performed according to the procedure described above for the empty CLNPs. The resulting NPs were termed BZL@CLNPs-CPP and BZL@CLNPs-PEG-PHIS-CPP.

The BZL loading into CLNPs was determined by immersing the drug-loaded CLNPs in ethanol for 30 min under vigorous stirring to degrade the CLNPs. After centrifugation at 13200 rpm for 5 min, the supernatant was collected in order to determine the BZL concentration by using high-performance liquid chromatography (HPLC; Agilent 1100 series, Agilent Technologies, USA). The experimental conditions used for quantification of the loaded BZL are described in detail in **Table S1** (25)**.**

4.9. *In vitro* Release Studies

BZL was used to evaluate the in vitro release profiles of free BZL, BZL@CLNPs, BZL@CLNPs-CPP and BZL@CLNPs-PEG-PHIS-CPP, performed in sink conditions in two different buffers: 1× HBSS–MES (HBSS–MES, pH 5.5) and HBSS–HEPES (pH 7.4), with 2% (v/v) of Tween 80. For that, 70 µg of pure BZL and 250 µg of BZL-loaded CLNPs were immersed in 60 mL and 20 mL of release media, respectively, and the samples were stirred at 150 rpm and 37 ºC. At the scheduled time intervals (2, 5, 10, 15, 20, 30, 60, 120, 180, 240, 360 min and 24 h), 200 µL of the release media were withdrawn and the same volume of fresh pre-heated release media was added, keeping the releasing volume constant. Afterwards, the samples were centrifuged at 13200 rpm for 3 min (room temperature, 25 ºC) and the supernatant was collected and analyzed in HPLC. The amount of BZL released was determined by measuring the BZL concentration using the HPLC method detailed in **Table S1**. The average values were obtained from at least three replicates.

4.10. Cell Antiproliferative Studies

The cell growth inhibition was evaluated after 24 h incubation at 37 ºC of pure BZL and BZL@CLNPs, BZL@CLNPs-CPP and BZL@CLNPs-PEG-PHIS-CPP with different cell lines. Briefly, MDA-MB-231, PC3-MM2, Caco-2 and EA.hy926 cells were

seeded in 96-well-plated at a density of 15000 cells per well and incubated overnight at 37 ºC to allow the cells to attach. After that, 100 µL of suspensions containing different concentrations of BZL-loaded CLNPs (5, 10, 25, 50 and 100 µg/mL) and the respective concentrations of pure BZL previously dissolved with 1% ethanol (1.6, 3.3, 8.2, 16.4 and 32.9 µM) in cell media were added to each well. Incubations with cell media and 1% (v/v) Triton X-100 were used as a positive and negative controls, respectively. A specific control for pure BZL was also added with the same amount of ethanol used in the dilutions. After the incubation, the number of viable cells in culture was determined using the CellTiter-Glo® luminescence cell viability assay kit (Promega Corporation, USA), and the luminescence was measured using a Varioskan Flash plate reader. All the experiments were performed at least in triplicate.

4.11. Statistical Analysis

The measured values are expressed by mean ± standard deviation (s.d.) of at least three independent experiments. One-way analysis of variance (ANOVA) with the Bonferroni's post hoc-test was used to estimate the significant difference with a probabilities set of $*p < 0.05$, $**p < 0.01$ and $***p < 0.001$, using the GraphPad Prism (GraphPad software Inc., CA, USA).

5. Results and Discussion

5.1. Carboxylation of Lignin

Carboxylated lignin was prepared to increase the amount of carboxylic groups on the lignin surface for further conjugation reactions. For that, the hydroxyl groups of native lignin were reacted with succinic anhydride, with DMAP as catalyst (76).The possible mechanism for the carboxylation reaction is shown in **Figure 5. 1-A**. First, the nucleophilic attack of DMAP on a carbonyl group of succinic anhydride leads to the formation of a tetrahedral intermediate, which is more activated towards a nucleophilic attack to the hydroxyl groups on lignin than the original anhydride. Then, the lignin hydroxyl groups react with the intermediate to give another intermediate that will collapse, and the pyridine group is eliminated to obtain carboxylated lignin (77)

To confirm the success of the carboxylation reaction, the ATR-FTIR spectra of CL and native lignin were compared and analyzed (**Figure 5. 1-B**). Both lignin and carboxylated lignin displayed the typical bands corresponding to the presence of different functional groups, such as alcoholic and phenolic –OH (3500–3100 cm-1), carbonyl groups (1600 cm^{-1}) and aromatic structure (1427–1512 cm^{-1}) (78). However, the CL showed a stronger absorption band at ca. 1720 cm^{-1} than the native lignin, mainly because of the stretching vibrations of C=O of the unconjugated –COOH groups. This can also be due to the stretching vibrations of C=O that derive from the ketone group situated at β-location, which is also present in the native lignin, represented by the shoulder in the same region of the spectrum (78). The description of the main lignin functional groups, their IR absorption bands and respective type of vibration are detailed in **Table S2** (78).

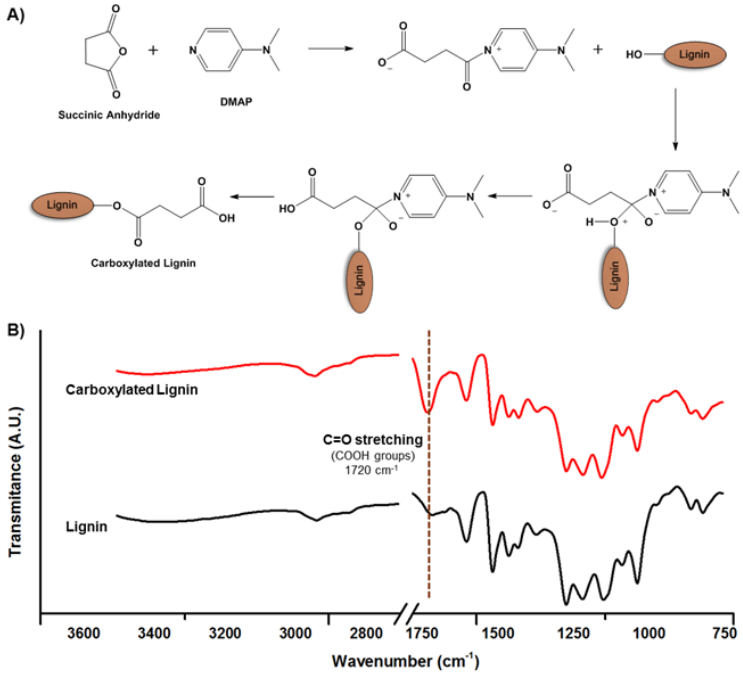

Figure 5. 1 - (A) Schematic representation of the lignin carboxylation reaction. (B) ATR-FTIR spectra of native lignin (black) and carboxylated lignin (red).

5.2. Characterization of Carboxylated Lignin Nanoparticles

After carboxylation of the native lignin, CLNPs dispersed in water were formed by solvent exchange, using the same dialysis method reported in previous studies (25,72,79). Using EDC/NHS coupling chemistry, the CLNPs were functionalized NH_2-PEG-PHIS to simultaneously increase the circulation in the bloodstream of the NPs due to the PEGylation effect, by preventing their opsonization, detection, and clearance by macrophages, and also to provide a pH-responsive behavior by using PHIS (80,81). In addition, the CLNPs were also modified by covalent binding of polyarginine R9 CPP, a small peptide with a high positive charge that allows the translocation through the negatively charged cellular plasma membrane (82). Afterwards, the bare and functionalized CLNPs were characterized by measuring their average size, PDI and ζ-potential (**Figure 5. 2-A and 5.2-B**). The bare CLNPs size was 240 ± 22 nm, while the CLNPs-CPP and CLNPs-PEG-PHIS-CPP presented and average size of 375 ± 22 nm and 373 ± 14 nm, respectively. A slight increase in the average size was observed for the

functionalized CLNPs as a result of the conjugation reactions. Regarding the size distribution of the three types of CLNPs, the PDI values were below 0.25, indicating a moderate dispersity of the resulting CLNPs. The size distribution and morphology of the prepared CLNPs were also studied by TEM (**Figure 5.2-C**). Even though the particles exhibited an average size similar to the values found by DLS, some discrepancies between the DLS and TEM measurements were observed, confirming the moderate dispersity of the prepared CLNPs. This phenomenon was previously reported in the literature, and it is explained by the fact that the DLS highlights the larger particles in the whole sample; but when observing the sample by TEM, it is possible to visualize some small particles that are not determined by DLS (25,83). In addition, the CLNPs showed symmetric and spherical shape, due to the appropriate interaction between the lignin and water during the solvent exchange process.

Regarding the surface charge, the ζ-potential value obtained for bare CLNPs was -36 ± 4 mV, because of the –COOH groups present on the surface of CLNPs (**Figure 5. 2-B**). However, a conversion of the ζ-potential to positive values was observed after the conjugations, where the CLNPs-CPP and CLNPs-PEG-PHIS-CPP showed 27 ± 10 and

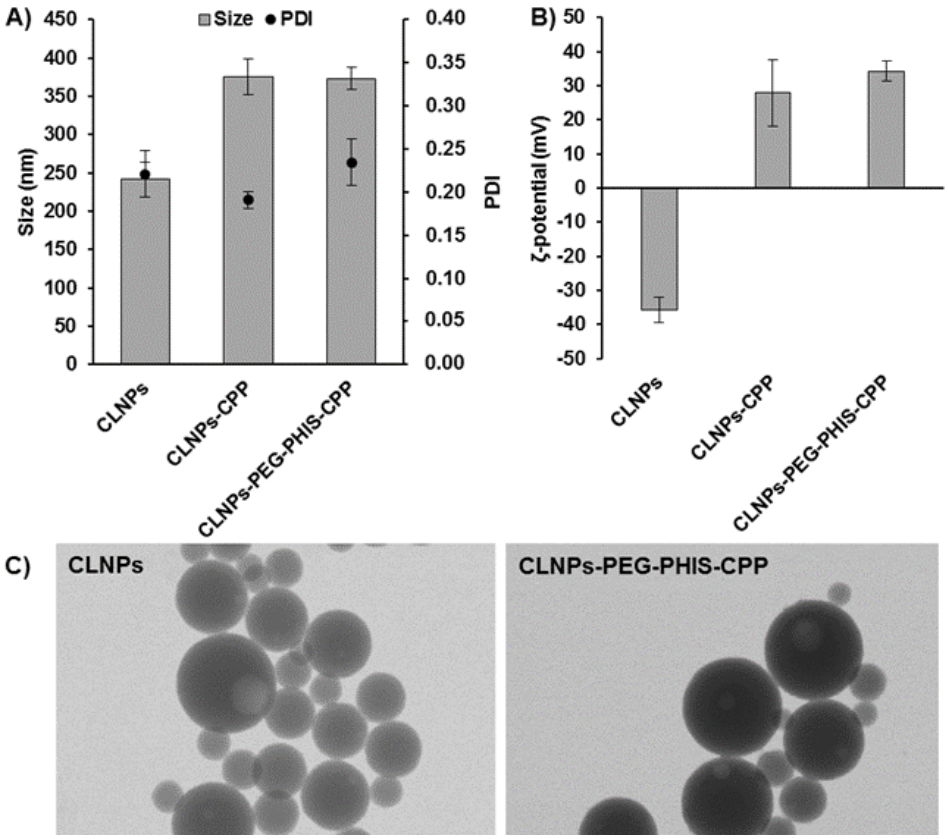

Figure 5. 2 - Characterization of CLNPs and functionalized CLNPs by: (A) measuring their average size and PDI; (B) ζ-potential, and (C) TEM images of CLNPs and CLNPs-PEG-PHIS-CPP.

34 ± 3 mV, respectively, suggesting that the reactions of CLNPs with NH_2-PEG-PHIS and CPP were successfully achieved. Both PHIS and CPP are positively charged due to the presence of $–NH_2$ groups.

Additionally, ATR-FTIR was performed to determine the chemical groups present on the surface of the particles and evaluate the differences between the bare CLNPs and the functionalized CLNPs (**Figure 5. 3**). For the undecorated CLNPs and conjugated CLNPs, the absorption band at around 1720 cm^{-1} was observed, because of the C=O stretching vibrations of the unconjugated –COOH groups. However, CLNPs-CPP and CLNPs-PEG-PHIS-CPP showed a characteristic band absorbing near 1670 cm^{-1}, corresponding to the C=O stretching vibrations of the amide bond (O=C–NH), with minor contributions from the out-of-phase C–N stretching vibration, the C–C–N deformation and the N–H in-plane bend (84,85). Simultaneously, a decrease in the intensity of the band at 1720 cm^{-1} was observed when compared to the bare CLNPs. Furthermore, a small peak at ca. 1640 cm^{-1} also appeared, which is assigned to the $–NH_2$ groups present on CPP and PHIS (86). The ATR-FTIR spectrum of the mixed CLNPs and PEG-PHIS (so-called physical mixing) was also evaluated in order to compare with the conjugated CLNPs-PEG-PHIS-CPP. In the physical mixing, the absorption bands were slightly different from the observed for the CLNPs. Furthermore, the characteristic band at 1670 cm^{-1} of the C=O stretching vibrations corresponding to the amide bond formation did not appear and a stronger band near 1640 cm^{-1} was present due to the NH_2 groups on the PHIS.

Thus, the ATR-FTIR spectra, together with the obtained ζ-potential values for the bare and conjugated CLNPs, suggested the success of the conjugation reactions.

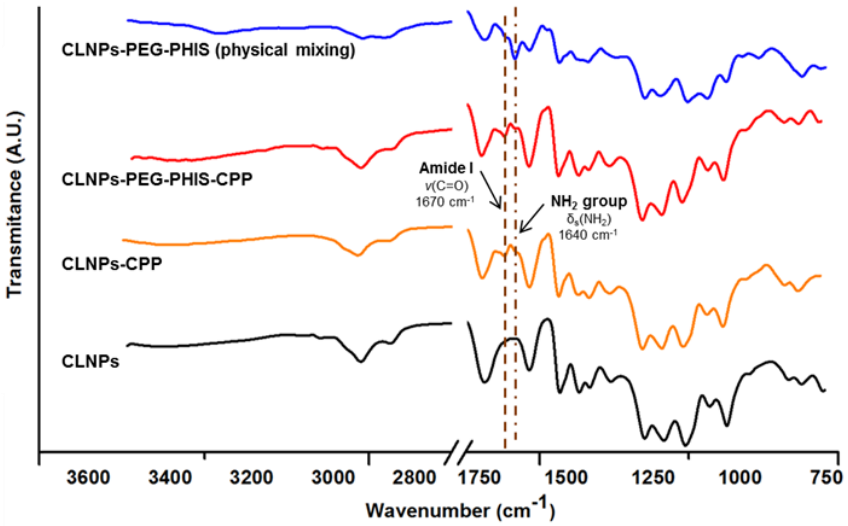

Figure 5. 3 - Characterization of bare CLNPs and functionalized CLNPs by ATR-FTIR

5.3. Stability of Carboxylated Lignin Nanoparticles

The extent and specificity of serum/plasma protein binding to the surface of the NPs in physiological environment is influenced by the composition, size, shape and surface chemistry of the particles (e.g., surface charge), affecting their biodistribution in the body (87). The long-term binding of proteins on the NPs leads to formation of a "hard corona", while the reversible binding of proteins that have faster exchange rates forms a "soft corona" (88). Therefore, the stability of the CLNPs was evaluated in biological media by measuring the changes on the size of the NPs. For that, the CLNPs were incubated in DMEM, supplemented with 10% of heated inactivated fetal bovine serum (FBS) and human plasma at 37 °C for 2 h (**Figure 5. 4**).

Concerning the stability of CLNPs in DMEM supplemented with 10% FBS, an increase of 200 nm in the CLNPs' size was observed during the first minutes of incubation, indicating some protein adsorption onto the NPs' surface due to the FBS proteins. However, the size of the bare CLNPs decreased to the initial size, whereas the size of the conjugated CLNPs was kept constant over time. Due to the positive charge of the conjugated CLNPs, the electrostatic effect between the NPs and the proteins of opposite surface charge can favor the formation of a soft corona that keeps constant over time (88,89). Regarding the human plasma, the size of the conjugated CLNPs had a higher increase than the bare CLNPs during the early minutes of incubation, which suggests a protein adsorption onto the CLNPs after contact with human plasma. After 10 min of

incubation, the size decreased substantially for the conjugated CLNPs due to the slow detachment of the adsorbed proteins that were weakly interacting with the hard protein corona layer. Here, the surface charge seems to play an important role in the interaction with the serum/plasma proteins (88,89). It is known that positively charged NPs have a short blood circulation half-life, because the proteins adsorbed on the surface of the NPs promote opsonization and, consequently, a rapid clearance from the bloodstream (88,90). Although there is PEG on the composition of the CLNPs-PEG-PHIS-CPP, the positive charge of the PHIS in outer part of the NPs can have a stronger effect than the PEG, or the PEG density on the surface of the NPs is not enough to limit the adsorption of proteins (91).

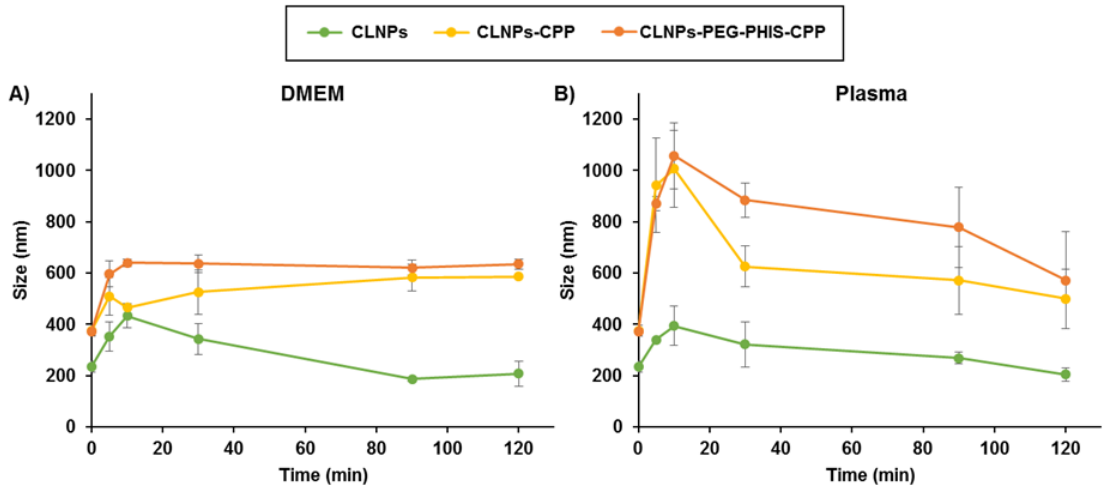

Figure 5. 4 - Effect on the size of CLNPs, CLNPs-CPP and CLNPs-PEG-PHIS-CPP after 2 h incubation in (A) DMEM supplemented with 10% of FBS and (B) human plasma at 37 °C. Errors bars represent mean ± s.d. (n = 3).

5.4. *In vitro* Cytotoxicity

Different NPs' properties (e.g., size, shape, and composition and surface charge) can affect the cell-NP interactions and, consequently, their cytotoxicity.(92,93)**.** In order to study the *in vitro* cytocompatibility of the prepared CLNPs, different concentrations of bare and functionalized CLNPs up to 500 µg/mL were incubated during 24 h with several cancer cell lines: MDA-MB-231 (**Figure 5. 5-A**), PC3-MM2 (**Figure 5. 5-B**), and Caco-2 (**Figure 5. 5-C**) cells. These cancer cell lines were selected based on the therapeutic effect of the selected cytotoxic compound in the treatment of breast, prostate and colorectal cancers, respectively (94,95). In addition to that, a non-tumor EA.hy926

endothelial cell line was also chosen to evaluate the cytotoxic effect of the different CLNPs in a healthy cell line (**Figure 5. 5-D**).

All the tested concentrations of CLNPs before and after functionalization showed a very good cytocompatibility after 24 h of incubation with more than 80% of cell viability, with exception for the highest concentration of CLNPs (250 and 500 µg/mL) after incubation with Caco-2 cells, which showed an increased toxicity to the cells. After conjugation with CPP, the surface charge of CLNPs changed from negative to positive values, and no statistically significant differences were observed when compared with the bare CLNPs, with the exception of the Caco-2 cells. Although some studies have been shown that the positively charged NPs can increase the interactions with the negatively charged cell membrane surface, others have reported that the surface charge of the NPs appears to play no role (96–98). The same trend was observed after conjugation of CLNPs with PEG-PHIS and CPP, which resulted in the production of positively charged NPs, without causing toxicity to the tested cell lines. Here, the effect of the PEGylation may be inhibiting the cell-NP interactions and the cellular uptake due to the steric hindrance (99).

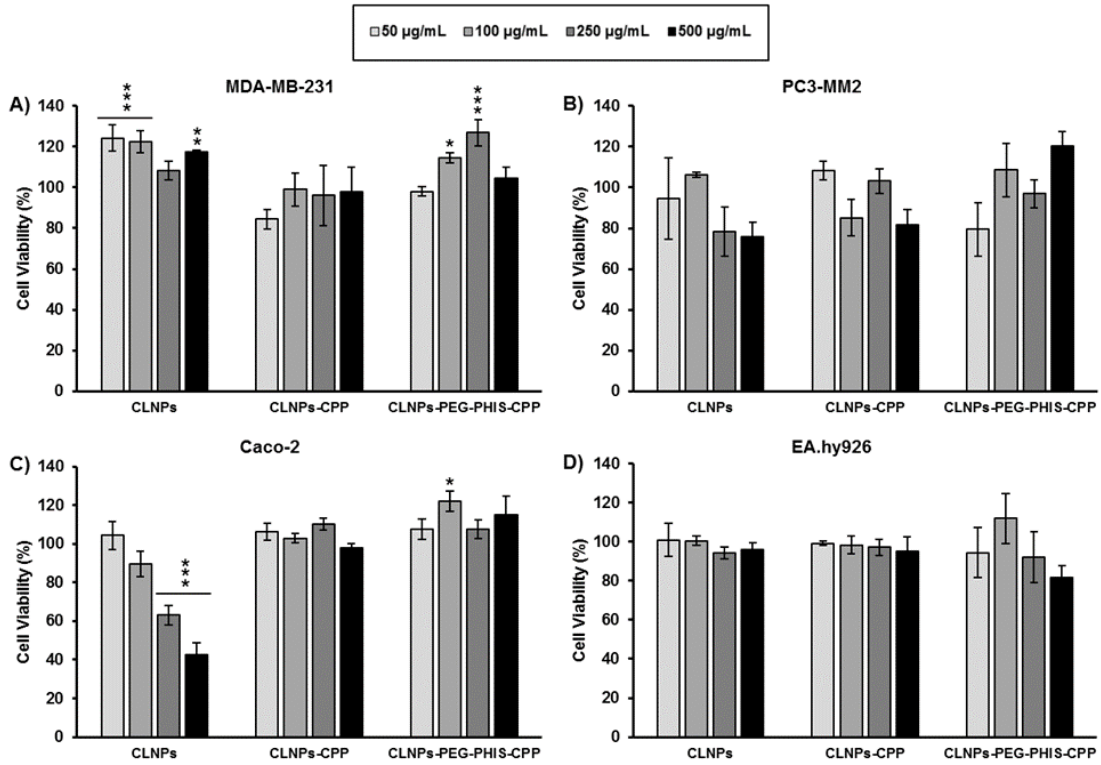

Figure 5. 5 - Cell viability of MDA-MB-231 (A), PC3-MM2 (B), Caco-2 (C) and EA.hy926 (D) cell lines after incubation with CLNPs, CLNPs-CPP and CLNPs-PEG-PHIS-CPP at different concentrations for 24 h at 37 °C. The viability was determined by the Cell Titer-Glo® luminescence assay and all data sets were compared to the positive control (different cell media). Errors bars represent the mean ± s.d. (n ≥ 3). The level of the significant differences was set at probabilities of *p < 0.05, **p < 0.01 and ***p < 0.001.

5.5. Loading of BZL and In Vitro Release Study

In this study, a poorly water-soluble cytotoxic agent (BZL) was used as a model drug to study the potential of the functionalized CLNPs as a drug delivery system. For that, the BZL-loaded CLNPs were prepared by dialysis method, and the conjugations with PEG-PHIS and/or CPP were carried out afterwards. The characterization of the BZL-loaded CLNPs is summarized in **Table 5. 1**. In general, the size of the CLNPs after loading was slightly higher than the empty CLNPs. BZL@CLNPs, BZL@CLNPs-CPP and BZL@CLNPs-PEG-PHIS-CPP presented an average size of 295 ± 25, 402 ± 24 and 438 ± 56 nm, respectively. With exception of BZL@CLNPs-PEG-PHIS-CPP, the PDI values of the BZL-loaded CLNPs were lower than 0.25, indicating again a moderate dispersity of the prepared CLNPs. In addition to that, the ζ-potential values of the CLNPs and drug-loaded CLNPs did not change significantly after loading.

The loading degree and encapsulation efficiency of BZL was determined by releasing the cargo after suspending the NPs in ethanol for 30 min and analyzing it by HPLC. The loading degree of BZL in the CLNPs, CLNPs-CPP and CLNPs-PEG-PHIS-CPP was 11 ± 1, 10 ± 1 and 9 ± 1%, respectively, decreasing along the conjugation reactions. Similarly, the encapsulation efficiency also decreased during the conjugations, being 57 ± 7, 50 ± 5 and 50 ± 10% for BZL@CLNPs, BZL@CLNPs-CPP and BZL@CLNPs-PEG-PHIS-CPP, respectively.

Table 5. 1 - Characterization of BZL-loaded CLNPs before and after the conjugation with PEG-PHIS and/or CPP in terms of average size, PDI, ζ-potential, loading degree (LD) and encapsulation efficiency (EE). Results as presented as mean ± s.d. (n ≥ 3).

Sample	Size (nm)	PDI	ζ-potential (mV)	LD (%)	EE (%)
BZL@CLNPs	295 ± 25	0.21 ± 0.04	–34 ± 3	11 ± 1	57 ± 7
BZL@CLNPs-CPP	402 ± 24	0.23 ± 0.10	20 ± 7	10 ± 1	50 ± 5
BZL@CLNPs-PEG-PHIS-CPP	438 ± 56	0.34 ± 0.03	42 ± 3	9 ± 1	50 ± 10

The release profiles of pure BZL and BZL-loaded CLNPs were evaluated in two different aqueous buffers, HBSS-MES (pH 5.5) and HBSS-HEPES (pH 7.4), mimicking the tumor microenvironment and the physiological pH, respectively (**Figure 5. 6-A and**

5. 6-B). To keep the sink conditions during the release, 2% (v/v) of Tween 80 was added to the release media.

For the pure BZL, the release of BZL at pH 5.5 was slightly slower than at pH 7.4, being ca. 26 and 47% after 6 h, but the dissolution of BZL reached a plateau around 48% after 24 h in both pH values tested. However, when loaded into CLNPs, the BZL dissolution was strongly improved, particularly at pH 5.5, in which it reached ca. 100% after 24 h. At pH 7.4, a decreased amount of BZL was released from the CLNPs after 24 h, when compared with the BZL released from the CLNPs at pH 5.5, which can be due to the precipitation or degradation of BZL.

The release of BZL from the three types of CLNPs in both pH-values presented the following rate: BZL@CLNPs > BZL@CLNPs-CPP > BZL@CLNPs-PEG-PHIS-CPP. Here, the functionalization of the CLNPs with the block copolymer or peptide seems to slightly slow down the release of BZL from the conjugated CLNPs, acting as a drug release barrier. Alternatively, ionic interactions between the drug and the attached block copolymer or peptide can also affect the release of BZL (100). In addition, the release of BZL from CLNPs showed a pH-responsive behavior, being released more efficiently at pH 5.5: the BZL@CLNPs-PEG-PHIS-CPP showed a sustained release of BZL when compared to the BZL@CLNPs and BZL@CLNPs-CPP. This can be due to the presence of a protonable nitrogen on the imidazole ring of PHIS that when it is protonated leads to a change on the conformation of the block-copolymer on the surface of the CLNPs, allowing the drug release (74,81). Overall, these nanosystems showed an enhancement on the dissolution rate and a pH-responsive release of the tested hydrophobic cytotoxic BZL compound, by a diffusion mechanism through the lignin structure (25).

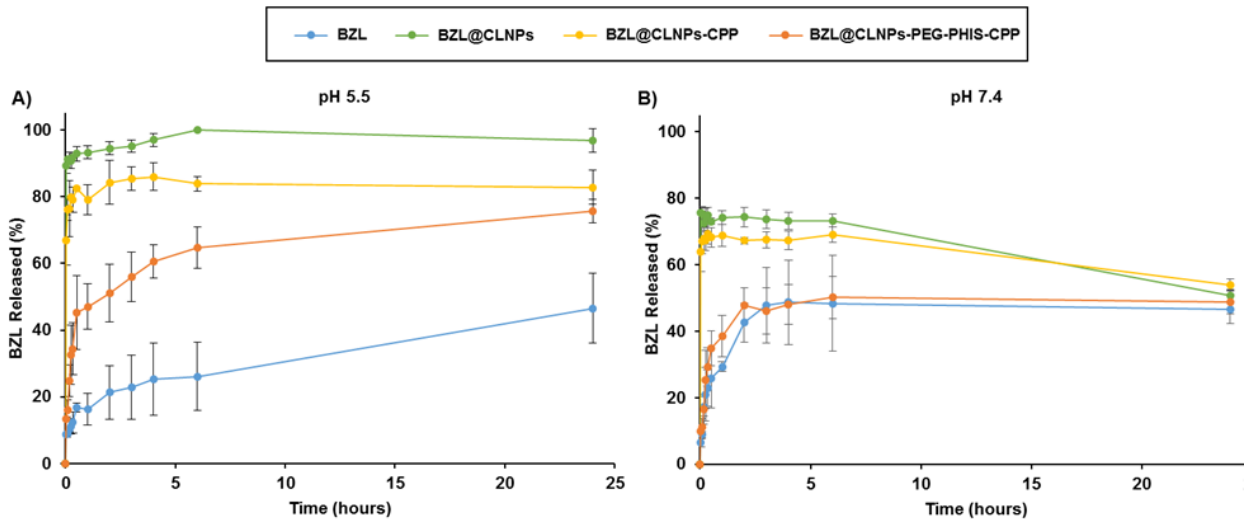

Figure 5. 6 - Release profiles of pure drug and drug-loaded CLNPs, CLNPs-CPP and CLNPs-PEG-PHIS-CPP in (A) HBSS–MES (pH 5.5) and (B) HBSS–HEPES (pH 7.4), containing 2% Tween 80 at 150 rpm and 37 ºC for 24 h. Errors bars represent the mean ± s.d. (n = 3).

5.6. Cell Antiproliferative Study

The antiproliferative effect of the BZL-loaded CLNPs was studied after the loading capacity of BZL into CLNPs and their release profiles were evaluated. BZL inhibits the oncogenic Pim kinases that are often overexpressed in some solid tumors, including prostate and colon cancers, triggering the tumor development (73,94,95). Here, we used MDA-MB-231, PC3-MM2 and Caco-2 cells to represent the breast, prostate and colon cancers, respectively. Additionally, a non-tumor endothelial cell line (EA.hy926) was also tested in order to compare the toxicity caused by the BZL released from the CLNPs in a physiologic environment with the tumor microenvironment showed in cancer cells. For that, the growth inhibition effect of BZL-loaded CLNPs (at concentrations ranging from 5 to 100 µg/mL) was evaluated and compared with equal molar ratio of free BZL, a poorly water-soluble compound that was completely dissolved with 1% ethanol and diluted with cell culture media, after 24 h incubation (**Figure 5.7 A-D**). A similar trend on the antiproliferative effect of pure BZL and BZL-loaded CLNPs before and after functionalization was observed within the same cell line. Additionally, the half maximal inhibitory concentration (IC_{50}) values were calculated for all the cell lines and are represented in **Figure 5.7 E** and detailed in **Table S3**. In general, when incubated with the three cancer cell lines, the CLNPs were more effective in decreasing the cell viability than the pure BZL, with reduced IC_{50}. Here, the antiproliferative effect of the BZL@CLNPs showed the following general rate in cancer cell lines: BZL@CLNPs-PEG-PHIS-CPP > BZL@CLNPs > BZL@CLNPs-CPP > pure BZL. The BZL@CLNPs-PEG-PHIS-CPP presented a smaller IC_{50} (< 23.4 µM) than BZL@CLNPs (< 25.8 µM), BZL@CLNPs-CPP (< 29.1 µM) and pure BZL (< 37.5 µM). However, after incubation with EA.hy926 cells, the BZL@CLNPs-PEG-PHIS-CPP showed the highest IC_{50} (45.1 µM), whereas the IC_{50} values for pure BZL, BZL@CLNPs and BZL@CLNPs-CPP were approximately 31 µM. This suggests that the coating with PEG-PHIS is decreasing the BZL release from the CLNPs-PEG-PHIS-CPP in physiologic environment, inducing less toxic effects to the normal cells.

Overall, the BZL-loaded CLNPs showed an effective cell growth inhibition in all the cancer cell lines tested without using an organic solvent (*e.g.*, ethanol) to solubilize the BZL, due to the enhanced solubility of BZL when loaded into CLNPs.

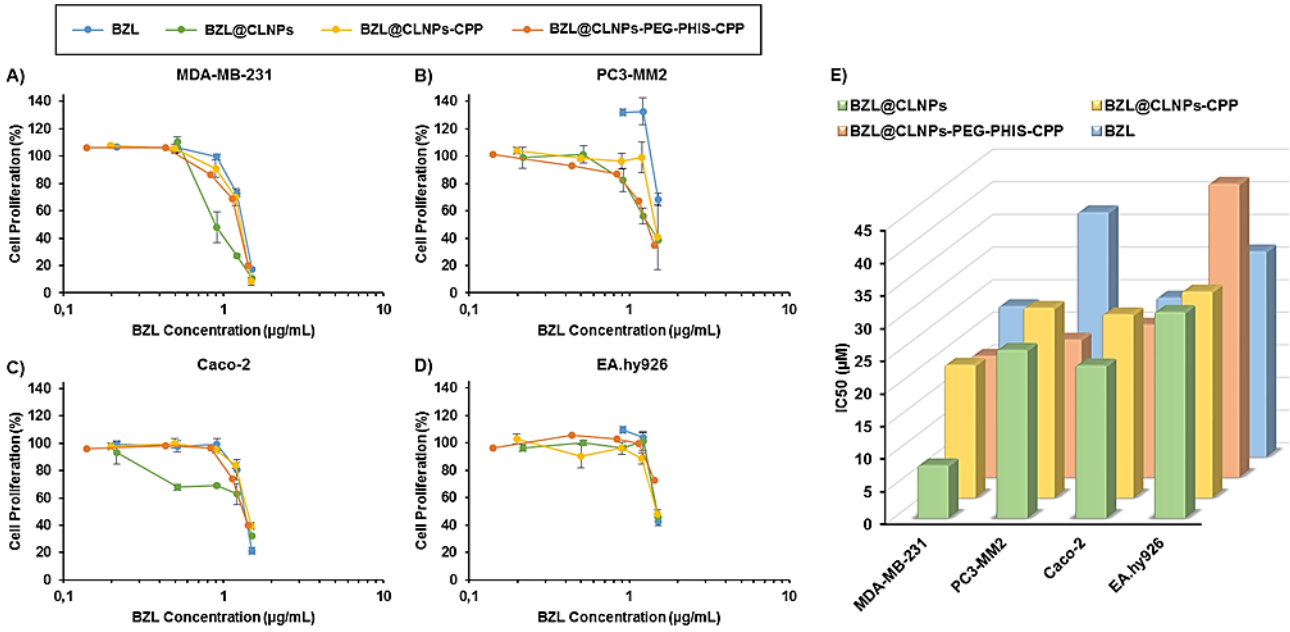

Figure 5. 7 - Antiproliferative studies of (A) MDA-MB-231, (B) PC3-MM2, (C) Caco-2 and (D) EA.hy926 cell lines treated with pure BZL, previously dissolved with 1% ethanol, and BZL-loaded CLNPs. The samples were incubated at different concentrations in complete media, for 24 h at 37 °C. Errors bars represent the mean ± s.d. ($n \geq 3$). (E) IC_{50} values obtained for BZL (blue), BZL@CLNPs (green), BZL@CLNPs-CPP (yellow) and BZL@CLNPs-PEG-PHIS-CPP (orange) after 24 h of incubation with the different cell lines

6. Conclusions

In the present study, we have developed and characterized three innovative CLNPs: the bare CLNPs and two functionalized CLNPs (CLNPs-CPP and CLNPs-PEG-PHIS-CPP), which presented round shape and moderately uniform dispersity. The success of the conjugation reactions was confirmed by ATR-FTIR and by the alteration of the ζ-potential values of the CLNPs after the conjugation reactions. All the CLNPs exhibited low cytotoxicity at concentrations up to at least 250 μg/mL in different cell lines at 24 h incubation. Concerning the drug loading capacity, our results indicate both the potential of using functionalized CLNPs to load a poorly water-soluble cytotoxic agent (BZL), and also the enhancement of its release profile in both pH 5.5 and 7.4, with higher release rates at acidic pH. Furthermore, the antiproliferative effect of BZL in the different cancer cell lines was enhanced after loading into CLNPs-PEG-PHIS-CPP, with lower IC_{50} values than BZL@CLNPs, BZL@CLNPs-CPP and pure BZL. However, when incubated with EA.hy926 cells, the BZL@CLNPs-PEG-PHIS-CPP showed the highest IC_{50}, (45.1 μM), suggesting that the coating with PEG-PHIS can decrease the release of BZL from the CLNPs-PEG-PHIS-CPP in physiologic environment, causing less toxic effects to the normal cells. Overall, the functionalized CLNPs showed interesting properties for drug delivery and biomedical applications, including biocompatibility, good stability in biological media, and capability to load hydrophobic drugs and sustain their release.

7. References

1. Pillai G, Ceballos-Coronel ML. Science and technology of the emerging nanomedicines in cancer therapy: A primer for physicians and pharmacists. SAGE Open Med [Internet]. 2013;1:2050312113513759. Available from: http:/ http://dx.doi.org/10.1177/2050312113513759

2. Astruc D. Introduction to nanomedicine. Molecules [Internet]. 2016;21(4). Available from: http://dx.doi.org/10.3390/molecules21010004

3. Nikalje AP. Nanotechnology and its Applications in Medicine. Med Chem (Los Angeles) [Internet]. 2015;5(2):81–9. Available from: http://dx.doi.org/10.4172/2161-0444.1000247

4. Bhattacharyya D, Singh S, Satnalika N. Nanotechnology , Big things from a Tiny World : a Review. Sci Technol [Internet]. 2009;2(3):29–38. Available from: http://www.ida.liu.se/~TGTU51/articles/MPN-paper.pdf

5. Salata O. Applications of nanoparticles in biology and medicine. J Nanobiotechnology [Internet]. 2004;2(3):1–6. Available from: http:// dx.doi.org/ 10.1186/1477-3155-2-3

6. Silva Adaya D, Aguirre-Cruz L, Guevara J, Ortiz-Islas E. Nanobiomaterials' applications in neurodegenerative diseases. J Biomater Appl [Internet]. 2017;31(7):953–84. Available from: dx.doi.org/ 10.1177/0885328216659032

7. Gharagozloo M, Majewski S, Foldvari M. Therapeutic applications of nanomedicine in autoimmune diseases: From immunosuppression to tolerance induction. Nanomedicine Nanotechnology, Biol Med [Internet]. 2015;11(4):1003–18. Available from: http://dx.doi.org/10.1016/j.nano.2014.12.003

8. Dolati S, Babaloo Z, Jadidi-Niaragh F, Ayromlou H, Sadreddini S, Yousefi M. Multiple sclerosis: Therapeutic applications of advancing drug delivery systems. Biomed Pharmacother [Internet]. 2017;86:343–53. Available from: http:// http://dx.doi.org/10.1016/j.biopha.2016.12.010

9. Kratz J, Chaddha A, Bhattacharjee S, Goonewardena S. Atherosclerosis and Nanotechnology: Diagnostic and Therapeutic Applications. Cardiovasc Drugs Ther [Internet]. 2016;30(1):33–9. Available from: http:// http://dx.doi.org/10.1007/s10557-016-6649-2

10. Karimi M, Zare H, Bakhshian Nik A, Yazdani N, Hamrang M, Mohamed E, et al. Nanotechnology in diagnosis and treatment of coronary artery disease. Nanomedicine (Lond) [Internet]. 2016;11(5):513–30. Available from: http:// http://dx.doi.org/ 10.2217/nnm.16.3

11. Barry M, Pearce H, Cross L, Tatullo M, Gaharwar AK. Advances in Nanotechnology for the Treatment of Osteoporosis. Curr Osteoporos Rep [Internet]. 2016;14(3):87–94. Available from: http://dx.doi.org/10.1007/s11914-016-0306-3

12. Parchi PD, Vittorio O, Andreani L, Battistini P, Piolanti N, Marchetti S, et al. Nanoparticles for tendon healing and regeneration: Literature review. Front Aging Neurosci [Internet]. 2016;8:1–5. Available from:

http://dx.doi.org/10.3389/fnagi.2016.00202

13. Vieira DB, Gamarra LF. Advances in the use of nanocarriers for cancer diagnosis and treatment. Einstein (São Paulo) [Internet]. 2016;14(1):99–103. Available from: http://dx.doi.org/10.1590/S1679-45082016RB3475

14. Siddiqui IA, Sanna V. Impact of nanotechnology on the delivery of natural products for cancer prevention and therapy. Mol Nutr Food Res [Internet]. 2016;60:1330–41. Available from: http://dx.doi.org/10.1002/mnfr.201600035

15. World Health Organization, Cancer Research UK. World cancer factsheet. World Heal Organ [Internet]. 2014. . Available from: http://www.cancerresearchuk.org/sites/default/files/cs_report_world.pdf

16. World Health Organization. Worldwide Cancer Incidence. World Heal Organ World Heal Organ [Internet] 2014. Available from: https://www.cancerresearchuk.org/sites/default/files/cs_infog_world_inc.pdf

17. World Health Organization. Worldwide Cancer Mortality. World Heal Organ [Internet]. 2014. Available from: http://www.cancerresearchuk.org/sites/default/files/cs_infog_world_mort.pdf

18. Mitra A, Agrahari1 V, Mandal A, Kishore, Cholkar Chandramouli N, Shah S, Joseph M, et al. Novel Delivery Approaches for Cancer Therapeutics. J Control Release [Internet] . 2015;219:248–68. Available from: http://dx.doi.org/10.1016/j.jconrel.2015.09.067

19. Bazak R, Houri M, Achy S El, Kamel S, Refaat T. Cancer active targeting by nanoparticles: a comprehensive review of literature. J Cancer Res Clin Oncol [Internet] . 2015;141(5):769–84. Available from: http://dx.doi.org/10.1007/s00432-014-1767-3

20. Prabhu RH, Patravale VB, Joshi MD. Polymeric nanoparticles for targeted treatment in oncology: Current insights. Int J Nanomedicine [Internet]. 2015;10:1001–18. Available from: http://dx.doi.org/10.2147/IJN.S56932

21. Bazak R, Houri M, Achy S El, Hussein W, Refaat T. Passive targeting of nanoparticles to cancer: A comprehensive review of the literature. Mol Clin Oncol [Internet]. 2014;2(6):904–8. Available from: http://dx.doi.org/10.3892/mco.2014.356

22. Masood F. Polymeric nanoparticles for targeted drug delivery system for cancer therapy. Mater Sci Eng C [Internet]. 2016;60:569–78. Available from: http://dx.doi.org/10.1016/j.msec.2015.11.067

23. Vinardell MP, Mitjans M. Lignins and Their Derivatives with Beneficial Effects on Human Health. Int J Mol Sci [Internet]. 2017;18:1219. Available from: http://dx.doi.org/10.3390/ijms18061219

24. Pollegioni L, Tonin F, Rosini E. Lignin-degrading enzymes. FEBS J [Internet]. 2015;282(7):1190–213. Available from: http://dx.doi.org/10.1111/febs.13224.

25. Figueiredo P, Lintinen K, Kiriazis A, Hynninen V, Liu Z, Ramos TB, et al. *In vitro* evaluation of biodegradable lignin-based nanoparticles for drug delivery and enhanced antiproliferation effect in cancer cells. Biomaterials [Internet] . 2017;121:97–108. Available from:

http://dx.doi.org/10.1016/j.biomaterials.2016.12.034

26. Rudramurthy GR, Swamy MK, Sinniah UR, Ghasemzadeh A. Nanoparticles: Alternatives against drug-resistant pathogenic microbes. Molecules [Internet]. 2016;21(7):1–30. Available from: http://dx.doi.org/ 10.3390/molecules21070836

27. Torres-Sangiao E, Holban AM, Gestal MC. Advanced nanobiomaterials: Vaccines, diagnosis and treatment of infectious diseases. Molecules [Internet]. 2016;21(7):1–22. Available from: http://dx.doi.org/10.3390/molecules21070867

28. Selby LI, Cortez-Jugo CM, Such GK, Johnston APR. Nanoescapology: progress toward understanding the endosomal escape of polymeric nanoparticles. Wiley Interdiscip Rev Nanomedicine Nanobiotechnology [Internet]. 2017;e1452. Available from: http://dx.doi.org/10.1002/wnan.1452

29. Kapse-Mistry S, Govender T, Srivastava R, Yergeri M. Nanodrug delivery in reversing multidrug resistance in cancer cells. Front Pharmacol [Internet]. 2014;5 JUL(July):1–22. Available from: http://dx.doi.org/10.3389/fphar.2014.00159

30. Kendall MAF. Drug Delivery. Vol. 197, Vaccine[Internet]. 2009. Available from: http://www.springerlink.com/index/10.1007/978-3-642-00477-3

31. Nagavarma BVN, Yadav HKS, Ayaz A, Vasudha LS, Shivakumar HG. Different techniques for preparation of polymeric nanoparticles- A review. Asian J Pharm Clin Res [Internet] . 2012;5(SUPPL. 3):16–23. Available from: http://dx.doi.org/

32. Nasir A, Kausar A, Younus A. A Review on Preparation, Properties and Applications of Polymeric Nanoparticle-Based Materials. Polym Plast Technol Eng [Internet]. 2014;54(4):325–41. Available from: http://dx.doi.org/10.1080/03602559.2014.958780

33. Ganesh K, Archana D. Review Article on Targeted Polymeric Nanoparticles : An Overview [Internet] . Am J Adv Drug Deliv. 2013;3(3):196–215. Available from: http://www.imedpub.com/articles/review-article-on-targeted-polymeric nanoparticles-an-overview.pdf

34. Murthy SK. Nanoparticles in modern medicine: state of the art and future challenges. Int J Nanomedicine [Internet]. 2007;2(2):129–41. Available from: http://www.pubmedcentral.nih.gov/articlerender.fcgi?artid=2673971&tool=pmcentrez&rendertype=abstract

35. Roy Chowdhury M, Schumann C, Bhakta-Guha D, Guha G. Cancer nanotheranostics: Strategies, promises and impediments. Biomed Pharmacother [Internet]. 2016;84:291–304. Available from: http://dx.doi.org/10.1016/j.biopha.2016.09.035

36. Mahapatro A, Singh DK. Biodegradable nanoparticles are excellent vehicle for site directed in-vivo delivery of drugs and vaccines. J Nanobiotechnology [Internet]. 2011;9(1):55. Available from: http://dx.doi.org/10.1186/1477-3155-9-55

37. Mirza AZ, Siddiqui FA. Nanomedicine and drug delivery: a mini review. Int Nano Lett [Internet]. 2014;4(1):94. Available from: http://dx.doi.org/10.1007/s40089-014-0094-7

38. Khodabandehloo H, Zahednasab H, Hafez AA. Nanocarriers Usage for Drug Delivery in Cancer Therapy. Iran J Cancer Prev. [Internet]. 2016;9(2). Available

from: http://dx.doi.org/10.17795/ijcp-3966

39. Sercombe L, Veerati T, Moheimani F, Wu SY, Sood AK, Hua S. Advances and challenges of liposome assisted drug delivery. Front Pharmacol. [Internet]. 2015;6:1–13. Available from: http://dx.doi.org/10.3389/fphar.2015.00286

40. Kilcoyne A, Harisinghani MG, Mahmood U. Prostate Cancer Imaging and Therapy: Potential Role of Nanoparticles. J Nucl Med [Internet]. 2016;57(Supplement_3):105S–110S. Available from: http://dx.doi.org/10.2967/jnumed.115.170738

41. Jo SD, Ku SH, Won YY, Kim SH, Kwon IC. Targeted nanotheranostics for future personalized medicine: Recent progress in cancer therapy. Theranostics [Internet]. 2016;6(9):1362–77. Available from: http://dx.doi.org/10.7150/thno.15335

42. Islamian JP, Hatamian M, Rashidi MR. Nanoparticles promise new methods to boost oncology outcomes in breast cancer. Asian Pacific J Cancer Prev [Internet]. 2015;16(5):1683–6. Available from: http://dx.doi.org/10.7314/APJCP.2015.16.5.1683

43. Nounou MI, ElAmrawy F, Ahmed N, Abdelraouf K, Goda S, Syed-Sha-Qhattal H. Breast Cancer: Conventional Diagnosis and Treatment Modalities and Recent Patents and Technologies. Breast Cancer (Auckl) [Internet]. 2015;9(Suppl 2):17–34. Available from: http://dx.doi.org/10.4137/BCBCR.S29420

44. Ouvinha de Oliveira R, de Santa Maria LC, Barratt G. Nanomedicine and its applications to the treatment of prostate cancer. Ann Pharm Fr [Internet]. 2014;72(5):303–16. Available from: http://dx.doi.org/10.1016/j.pharma.2014.04.006

45. Strief DM. An overview of prostate cancer: diagnosis and treatment. Medsurg Nurs [Internet]. 2008;17(4):258–263, 269; quiz 264. Available from: https://www.cbuna.org/sites/default/files/download/members/unjarticles/2007/07dec/475.pdf

46. Edwards MS, Chadda SD, Zhao Z, Barber BL, Sykes DP. A systematic review of treatment guidelines for metastatic colorectal cancer. Color Dis [Internet]. 2012;14(2):31–47. Available from: http://dx.doi.org/10.1111/j.1463-1318.2011.02765.x

47. Bartos A, Bartos D, Szabo B, Breazu C, Opincariu I, Mironiuc A, et al. Recent achievements in colorectal cancer diagnostic and therapy by the use of nanoparticles. Drug Metab Rev [Internet]. 2016;2532:1–17. Available from: http://dx.doi.org/10.3109/03602532.2015.1130052

48. Laroui Hamed, Rakhya1 P, Xiao1 B, Viennois E, Merlin D. Nanotechnology in Diagnostics and Therapeutics for Gastrointestinal Disorders. Dig Liver Dis [Internet]. 2013;45(12)(1):995–1002. Available from: http://dx.doi.org/10.1016/j.dld.2013.03.019

49. Sun L, Wu Q, Peng F, Liu L, Gong C. Strategies of polymeric nanoparticles for enhanced internalization in cancer therapy. Colloids Surfaces B Biointerfaces [Internet]. 2015;135:56–72. Available from: http://dx.doi.org/10.1016/j.colsurfb.2015.07.013

50. Wang H, Yu J, Lu X, He X. Nanoparticle systems reduce systemic toxicity in cancer treatment. Nanomedicine (Lond) [Internet]. 2016;11(2):103–6. Available from: http://dx.doi.org/10.2217/nnm.15.166

51. Parveen S, Sahoo SK. Polymeric nanoparticles for cancer therapy. J Drug Target [Internet]. 2008;16:108–23. Available from: http://dx.doi.org/10.1080/10611860701794353

52. Niazi M, Zakeri-Milani P, Najafi Hajivar S, Soleymani Goloujeh M, Ghobakhlou N, Shahbazi Mojarrad J, et al. Nano-based strategies to overcome p-glycoprotein-mediated drug resistance. Expert Opin Drug Metab Toxicol [Internet]. 2016;12(9):1021–33. Available from: http://dx.doi.org/10.1080/17425255.2016.1196186

53. Li F, Zhou X, Zhou H, Jia J, Li L, Zhai S, et al. Reducing both pgp overexpression and drug efflux with anti-cancer gold-paclitaxel nanoconjugates. PLoS One [Internet]. 2016;11(7):1–16. Available from: http://dx.doi.org/10.1371/journal.pone.0160042

54. Malmo J, Sandvig A, Vårum KM, Strand SP. Nanoparticle Mediated P-Glycoprotein Silencing for Improved Drug Delivery across the Blood-Brain Barrier: A siRNA-Chitosan Approach. PLoS One [Internet]. 2013;8(1). Available from: http://dx.doi.org/10.1371/journal.pone.0054182

55. Kim J, Wilson D, Zamboni CG, Green and JJ. Targeted polymeric nanoparticles for cancer gene therapy. J Drug Target [Internet]. 2015;33(4):627–641. Available from: http://dx.doi.org/ 10.3109/1061186X.2015.1048519

56. Poon Z, Lee JB, Morton SW, Hammond PT. Controlling In Vivo Stability and Biodistribution in Electrostatically Assembled Nanoparticles for Systemic Delivery. Nano Lett [Internet]. 2011;11(5):2096–103. Available from: http://dx.doi.org/ 10.1021/nl200636r

57. Harris TJ, Green JJ, Fung PW, Langer R, Daniel G. Tissue-Specific Gene Delivery via Nanoparticle Coating. Biomaterials [Internet]. 2010;31(5):998–1006. Available from: http://dx.doi.org/10.1016/j.biomaterials.2009.10.012

58. Calvo-Flores FG, Dobado JA. Lignin as renewable raw material. ChemSusChem [Internet]. 2010;3(11):1227–35. Available from: http://dx.doi.org/10.1002/cssc.201000157

59. Duval A, Lawoko M. A review on lignin-based polymeric, micro- and nano-structured materials. React Funct Polym [Internet]. 2014;85:78–96. Available from: http://dx.doi.org/10.1016/j.reactfunctpolym.2014.09.017

60. Abdelaziz OY, Brink DP, Prothmann J, Ravi K, Sun M, Garc??a-Hidalgo J, et al. Biological valorization of low molecular weight lignin. Biotechnol Adv [Internet]. 2016;34(8):1318–46. Available from: http://dx.doi.org/10.1016/j.biotechadv.2016.10.001

61. Weng J-K, Chapple C. The origin and evolution of lignin biosynthesis. New Phytol [Internet]. 2010;187:273–85. Available from: http://dx.doi.org/10.1111/j.1469-8137.2010.03327.x

62. El Mansouri N-E, Yuan Q, Huang F. Synthesis and characterization of kraft lignin-

based epoxy resins. BioResources [Internet]. 2011;6(3):2647–62. Available from: http://ojs.cnr.ncsu.edu/index.php/BioRes/article/view/BioRes_06_3_2492_ElMansouri_YH_Synth_Char_Kraft%2BLignin_Epoxy_Resins/1047

63. Ragauskas AJ, Beckham GT, Biddy MJ, Chandra R, Chen F, Davis MF, et al. Lignin valorization: improving lignin processing in the biorefinery. Science [Internet]. 2014;344(6185):1246843. Available from: http://dx.doi.org/10.1126/science.1246843

64. Beckham GT, Johnson CW, Karp EM, Salvachúa D, Vardon DR. Opportunities and challenges in biological lignin valorization. Curr Opin Biotechnol [Internet]. 2016;42:40–53. Available from: http://dx.doi.org/10.1016/j.copbio.2016.02.030

65. Malutan T, Nicu R, Popa VI. Lignin modification by epoxidation. BioResources [Internet]. 2008;3(4):1371–6. Available from: http://ojs.cnr.ncsu.edu/index.php/BioRes/article/view/BioRes_03_4_1371_Malutan_NP_Lignin_Mod_Epoxidation

66. Pan H, Sun G, Zhao T. Synthesis and characterization of aminated lignin. Int J Biol Macromol [Internet]. 2013;59:221–6. Available from: http://dx.doi.org/10.1016/j.ijbiomac.2013.04.049

67. Konduri MK, Kong F, Fatehi P. Production of carboxymethylated lignin and its application as a dispersant. Eur Polym J [Internet]. 2015;70:371–83. Available from: http://dx.doi.org/10.1016/j.eurpolymj.2015.07.028

68. Lievonen M. Preparation and Characterization of Lignin Nanoparticles. Aalto University [Internet]; 2015. Available from: http://dx.doi.org/https://aaltodoc.aalto.fi/handle/123456789/15064

69. Beisl S, Miltner A, Friedl A. Lignin from micro- to nanosize: Production methods. Vol. 18, International Journal of Molecular Sciences [Internet] . 2017. Available from: http://dx.doi.org/10.3390/ijms18061244

70. Thorat AA, Dalvi S V. Liquid antisolvent precipitation and stabilization of nanoparticles of poorly water soluble drugs in aqueous suspensions: Recent developments and future perspective. Chem Eng J [Internet]. 2012;181–182:1–34. Available from: http://dx.doi.org/10.1016/j.cej.2011.12.044

71. Richter AP, Bharti B, Armstrong HB, Brown JS, Plemmons D, Paunov VN, et al. Synthesis and characterization of biodegradable lignin nanoparticles with tunable surface properties. Langmuir [Internet]. 2016;32(25):6468–77. Available from: http://dx.doi.org/10.1021/acs.langmuir.6b01088

72. Lievonen M, Valle-Delgado JJ, Mattinen M-L, Hult E-L, Lintinen K, Kostiainen M a., et al. Simple process for lignin nanoparticle preparation. Green Chem [Internet]. 2015;1416–22. Available from: http://dx.doi.org/10.1039/C5GC01436K

73. Kiriazis A, Vahakoski RL, Santio NM, Arnaudova R, Eerola SK, Rainio EM, et al. Tricyclic Benzo[cd]azulenes Selectively Inhibit Activities of Pim Kinases and Restrict Growth of Epstein-Barr Virus-Transformed Cells. PLoS One. 2013;8(2). Available from: http://dx.doi.org/10.1371/journal.pone.0055409

74. Herranz-Blanco B, Shahbazi MA, Correia AR, Balasubramanian V, Kohout T,

Hirvonen J, et al. pH-Switch Nanoprecipitation of Polymeric Nanoparticles for Multimodal Cancer Targeting and Intracellular Triggered Delivery of Doxorubicin. Adv Healthc Mater [Internet]. 2016;5(15):1904–16. Available from: http://dx.doi.org/10.1002/adhm.201600160

75. Figueiredo P, Balasubramanian V, Shahbazi MA, Correia A, Wu D, Palivan CG, et al. Angiopep2-functionalized polymersomes for targeted doxorubicin delivery to glioblastoma cells. Int J Pharm [Internet]. 2016;511(2):794–803. Available from: http://dx.doi.org/10.1016/j.ijpharm.2016.07.066

76. Yang Q, Pan X. Correlation Between Lignin Physicochemical Properties and Inhibition to Enzymatic Hydrolysis of Cellulose. 2015;(December):1213–24. Available from: http://dx.doi.org/10.1002/bit.25903

77. Liu CF, Zhang AP, Li WY, Sun RC. Chemical Modification of Cellulose with Succinic Anhydride in Ionic Liquid with or without Catalysts. InTech [Internet]. 2010. 5:81-95. Available from: http://dx.doi.org/10.5772/14894

78. Ahvazi B, Cloutier E, Wojciechowicz O, Ngo TD. Lignin Profiling : A Guide for Selecting Appropriate Lignin as Precursors in Biomaterials Development. ACS Sustainable Chem [Internet]. 2016;4(10):5090–5105. Available from: http://dx.doi.org/10.1021/acssuschemeng.6b00873

79. Lintinena K, Latikkab M, Sipponen MH, Rasb RHA, Österberg M, Kostiainena MA. Structural Diversity in Metal-Organic Nanoparticles Based on Iron Isopropoxide Treated Lignin. RSC Adv [Internet]. 2016;6:31790–6. Available from: http://dx.doi.org/10.1039/C6RA03865D

80. Jokerst Jesse, Lobovkina T, Zare RN, Gambhir SS. Nanoparticle PEGylation for imaging and therapy. Nanomedicine (Lond) [Internet]. 2011;6(4):715–728. Available from: http://dx.doi.org/10.2217/nnm.11.19

81. Seong E, Joon H, Na K, Han Y. Poly (L -histidine)– PEG block copolymer micelles and pH-induced destabilization. J Control Release [Internet]. 2003;90:363–74. Available from: http://dx.doi.org/10.1016/S0168-3659(03)00205-0

82. Regberg J, Srimanee A, Langel Ü. Applications of Cell-Penetrating Peptides for Tumor Targeting and Future Cancer Therapies. Pharmaceuticals [Internet]. 2012;5:991–1007. Available from: http://dx.doi.org/10.3390/ph5090991

83. Durfee PN, Lin Y, Dunphy DR, Mun J, Butler KS, Humphrey KR, et al. Mesoporous Silica Nanoparticle-Supported Lipid Bilayers (Protocells) for Active Targeting and Delivery to Individual Leukemia Cells. ACS Nano. 2016;;10(9):8325-45Available from: http://dx.doi.org/10.1021/acsnano.6b02819

84. Barth A. Infrared spectroscopy of proteins. Biochim Biophys Acta [Internet]. 2007;1767:1073–101. Available from: http://dx.doi.org/10.1016/j.bbabio.2007.06.004

85. Kumar V, Nath G, Kotnala RK, Saxena PS, Srivastava A. Biofunctional magnetic nanotube probe for recognition and separation of specific bacteria from a mixed culture. RSC Adv [Internet]. 2013;3:14634–41. Available from: http://dx.doi.org/10.1039/C3RA42307G

86. Nawrotek K, Tylman M, Rudnicka K, Balcerzak J. Chitosan-based hydrogel implants enriched with calcium ions intended for peripheral nervous tissue regeneration. Carbohydr Polym [Internet] 2016;136:764–71. Available from: http://dx.doi.org/10.1016/j.carbpol.2015.09.105

87. Aggarwal P, Hall JB, Mcleland CB, Dobrovolskaia MA, Mcneil SE. Nanoparticle interaction with plasma proteins as it relates to particle biodistribution, biocompatibility and therapeutic efficacy. Adv Drug Deliv Ver [Internet]. 2013;61(6):428–37. Available from: http://dx.doi.org/10.1016/j.addr.2009.03.009

88. Saptarshi SR, Duschl A, Lopata AL. Interaction of nanoparticles with proteins : relation to bio-reactivity of the nanoparticle. 2013;1–12. Available from: http://dx.doi.org/10.1186/1477-3155-11-26

89. Sakulkhu U, Mahmoudi M, Maurizi L, Coullerez G, Hofmann-amtenbrink M, Vries M, et al. Significance of surface charge and shell material of superparamagnetic iron oxide nanoparticle (SPION) based core/shell nanoparticles on the composition of the protein corona. Biomater Sci [Internet]. 2014;3:265–78. Available from: http://dx.doi.org/10.1039/c4bm00264d

90. Alexis F, Pridgen E, Molnar LK, Farokhzad OC. Factors Affecting the Clearance and Biodistribution of Polymeric Nanoparticles. Mol Pharm. 2008;5(4):505–15. Available from: http://dx.doi.org/10.1021/mp800051m

91. Veronese FM, Mero A. The Impact of PEGylation on Biological Therapies. BioDrugs [Internet]. 2008;22(5):315-29. Available from: http://dx.doi.org/https://www.ncbi.nlm.nih.gov/pubmed/18778113

92. Nel AE, Mädler L, Velegol D, Xia T, Hoek EM V, Somasundaran P, et al. Understanding biophysicochemical interactions at the nano–bio interface. Nat Publ Gr [Internet]. 2009;8(7):543–57. Available from: http://dx.doi.org/10.1038/nmat2442

93. Albanese A, Tang PS, Chan WCW. The Effect of Nanoparticle Size , Shape , and Surface Chemistry on Biological Systems. Annu Rev Biomed Eng [Internet]. 2012;14:1-16. Available from: http://dx.doi.org/10.1146/annurev-bioeng-071811-150124

94. Shah N, Pang B, Yeoh KG, Thorn S, Chen CS, Lilly MB, et al. Potential roles for the PIM1 kinase in human cancer - A molecular and therapeutic appraisal. Eur J Cancer [Internet]. 2008;44(15):2144–51. Available from: http://dx.doi.org/10.1016/j.ejca.2008.06.044

95. Brault L, Gasser C, Bracher F, Huber K, Knapp S, Schwaller J. Pim serine/threonine kinases in the pathogenesis and therapy of hematologic malignancies and solid cancers. Haematologica. 2010;95(6):1004–15. Available from: http://dx.doi.org/10.3324/haematol.2009.017079

96. Kong B, Seog JH, Graham L, Lee SB. Experimental considerations on the cytotoxicity of nanoparticles. Nanomedicine [Internet]. 2011;6(5):929–41. Available from: http://dx.doi.org/10.2217/nnm.11.77

97. Fröhlich E. The role of surface charge in cellular uptake and cytotoxicity of medical nanoparticles. Int J Nanomedicine [Internet]. 2012;7:5577–91. Available from: http://dx.doi.org/10.2147/IJN.S36111

98. Mura S, Hillaireau H, Nicolas J, Droumaguet B Le, Gueutin C, Tsapis N, et al. Influence of surface charge on the potential toxicity of PLGA nanoparticles towards Calu-3 cells. Int J Nanomedicine [Internet]. 2011;6:2591–605. Available from: http://dx.doi.org/10.2147/IJN.S24552

99. Hatakeyama H, Akita H, Harashima H. Polyethyleneglycol : A Classical but Innovative Material The Polyethyleneglycol Dilemma : Advantage and Disadvantage of PEGylation of Liposomes for Systemic Genes and Nucleic Acids Delivery to Tumors. Biol Pharm Bull [Internet]. 2013;36:892–9. Available from: http://dx.doi.org/10.1248/bpb.b13-00059

100. Singh R, Jr. JWL. Nanoparticle-based targeted drug delivery. Exp Mol Pathol [Internet]. 2009;86(3):215–23. Available from: http://dx.doi.org/10.1016/j.yexmp.2008.12.004

8. Supporting Information

8.1. Materials and Cell Culturing

THF, HEPES and 2-(N-morpholino) ethanesulfonic acid (MES) were purchased from Sigma-Aldrich®, USA. Culture flasks were purchased from Corning Inc., USA. DMEM, Roswell Park Memorial Institute 1640 medium (RPMI), heat inactivated fetal bovine serum (FBS), L-glutamine (200 mM), non-essential amino acids (NEAA), penicillin (100 IU/mL), streptomycin (100 mg/mL), sodium pyruvate (100 mM) and trypsin (2.5%) were acquired from HyClone Waltham, USA. Dulbecco's phosphate buffer saline (10× PBS) and Hank's balanced salt solution (10× HBSS) were purchased from Life Technologies Gibco® (Carlsbad, CA, USA).

Human umbilical vein cell line (EA.hy926), human mammary carcinoma cell line (MDA-MB-231), human prostate cancer cell line (PC3-MM2) and human colorectal adenocarcinoma cell line (Caco-2) were obtained from American Type Culture Collection (ATCC), USA. The EA.hy926, PC3-MM2 and Caco-2 cells were incubated in DMEM, and the MDA-MB-231 cells were incubated with RPMI, supplemented with 10% FBS, 1% NEAA, 1% L-glutamine and 1% penicillin-streptomycin in 75 cm2 flasks. EA.hy926 medium was also supplemented with 1% sodium pyruvate. Cells were maintained in an incubator (BB 16 gas incubator, Heraeus Instruments GmbH) at 37 ºC, 5% CO2 and 95% relative humidity.

8.2. Synthesis of Poly(Ethylene Glycol)-Block-Poly(ι-Histidine) (NH_2-PEG-PHIS)

The block copolymers were synthesized by direct coupling of the amine group of PHIS with the succinimidyl ester activated carboxylic group from Boc-NH-PEG-NHS (**Figure S1 A**). For that, PHIS was dissolved in 10 mM of HEPES to a concentration of 2 mg/mL and the pH adjusted to 6.5. Two equivalents of Boc-NH-PEG-NHS were added to the solution with stirring. The reaction atmosphere was replaced with nitrogen gas in a round-bottom flask under stirring overnight. Then, the product of the reaction was purified by dialysis against deionized water, using a dialysis bag (MWCO of 8–10 kDa),

replacing the exchange medium after 2, 4, 6, 12, 24, and 48 h. Subsequently, the purified product was freeze-dried.

For the deprotection reaction, Boc-NH-PEG-PHIS was dissolved in a solution of 95% TFA to a concentration of 5 mg/mL, and stirred for 1.5 h (**Figure S1 B**). Then, the TFA was neutralized first by diluting it four times with deionized water, followed by addition of 0.5 M of NaOH until reaching a neutral pH. The entire process was carried out in ice. Finally, the product of the reaction was purified by dialysis against deionized water, using a dialysis bag (MWCO of 8–10 kDa), replacing the exchange medium after 2, 4, 6, 12, 24, and 48 h. Subsequently, the purified product NH2-PEG–PHIS was freeze-dried (74).

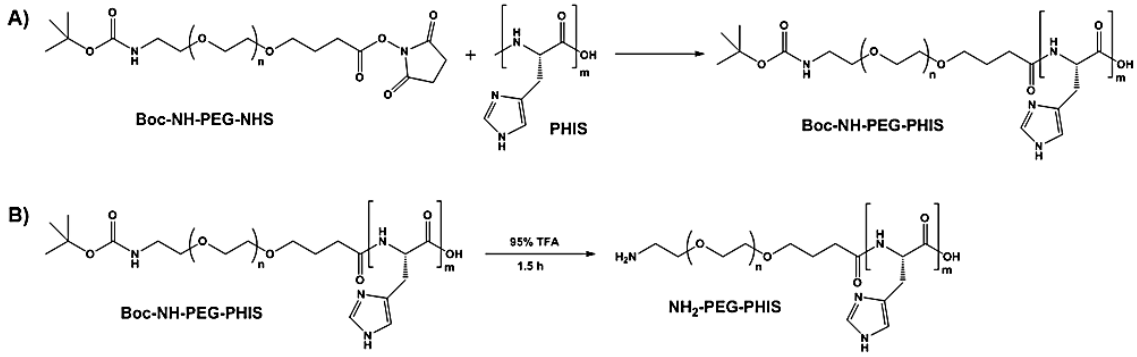

Figure S 1 – Schematic representation of the synthesis of Poly(Ethylene Glycol)-Block-Poly(ι-Histidine) (NH2-PEG-PHIS): A) Synthesis of Boc-NH-PEG-PHIS, and B) Deprotection of Boc-NH-PEG-PHIS

Table S 1 – HPLC conditions used in this study for quantification of the loaded and released BZL

	BZL
Mobile Phase (v/v)	Solution A: 0.1% Trifluoroacetic acid (pH 2.0) Solution B: Acetonitrile (35:65)
Column	Kinetex® C_{18}, 75×4.6 mm, 2.6 µm (Phenomenex, USA)
Flow Rate (mL/min)	1.0
Detection (UV, nm)	295
Injection Volume (µL)	15
Temperature (°C)	25

Table S 2 – Description of the main lignin functional groups: IR absorption bands and respective type of vibration (78)

IR band (cm^{-1})	Type of vibration
3500–3100	Stretching vibrations of alcoholic and phenolic –OH groups involved in hydrogen bonds
2920–2850	Stretching vibrations of C–H bonds in methoxyl group
1720	Stretching vibrations of C=O bonds at β location and in unconjugated –COOH group
1600	Stretching vibrations of C=O bonds at α- and γ-locations
1512	Aromatic ring vibrations
1465	
1427	
1269	Vibrations of guaiacyl rings and stretching vibrations of C–O bonds
1215	
1150	Deformation vibrations of C–H bonds in guaiacyl rings
1083	Deformation vibrations of C–O bonds in secondary alcohols and aliphatic ethers
1033	Deformation vibrations of C–H bonds in the aromatic rings and deformation vibrations of C–O bonds in primary alcohols
858	Deformation vibrations of C–H bonds in the aromatic rings
819	

Table S 3 – IC_{50} values of BZL determined for the different cell lines.

	BZL	**BZL@CLNPs**	**BZL@CLNPs-CPP**	**BZL@CLNPs-PEG-PHIS-CPP**
MDA-MB-231	23.1 ± 0.2	8.1 ± 1.0	20.4 ± 0.7	18.6 ± 0.2
PC3-MM2	37.5 ± 1.2	25.8 ± 3.7	29.1 ± 1.3	21.1 ± 1.1
Caco-2	24.4 ± 0.7	23.4 ± 2.3	28.1 ± 0.8	23.4 ± 0.9
EA.hy926	31.5 ± 1.0	31.6 ± 1.6	31.6 ± 0.7	45.1 ± 2.2